Crustal evolution of the Arabian–Nubian Shield

Insights from zircon geochronology and Nd–Hf–O isotopes

Fitsum Girum Yeshanew

Academic dissertation for the Degree of Doctor of Philosophy in Geology at Stockholm University to be publicly defended on Wednesday 20 September 2017 at 10.00 in De Geersalen, Geovetenskapens hus, Svante Arrhenius väg 14.

Abstract

The Arabian–Nubian Shield (ANS) represents a major site of juvenile Neoproterozoic crustal addition on Earth and documents Neoproterozoic tectonics bracketed by two supercontinent cycles, namely the fragmentation of Rodinia and the amalgamation of Gondwana. There is general consensus that the ANS formed by juvenile magmatic arc accretion and subsequent shield–wide post–tectonic magmatism. However, detailed understanding about the timing of events and the nature of magma sources in parts of the shield are lacking. To date, there are no isotopic data from the Paleozoic sedimentary sequences of the ANS, except those from the northern part. New zircon U–Pb, $\delta^{18}O$ and whole–rock Nd isotopes are presented for plutonic rocks from the eastern Ethiopia, Yemen and southernmost Arabian Shield in Saudi Arabia. This thesis also presents the first combined *in situ* zircon U–Pb–O–Hf isotope data on the Cambrian–Ordovician sandstones of the Arabian Shield. The results are used to elucidate the crustal evolution of these parts of the ANS and to evaluate terrane correlations. Specifically, the nature of crustal growth, i.e., relative proportions of juvenile magmatic additions vs. crustal reworking, nature of the magma source and mechanism of crust formation (plume material vs. subduction zone enrichment) and understanding the provenance of the Cambrian–Ordovician sandstone sequences were important research questions addressed.

The results from Paper I suggest that the eastern Ethiopian Precambrian basement is dominated by reworking of pre-Neoproterozoic supracrustal material unlike contemporaneous rocks in the remaining parts of Ethiopia— indicating the presence of two distinct lithospheric blocks of contrasting isotopic compositions in Ethiopia. Metamorphic age distributions suggest that the eastern Ethiopian block was amalgamated with the juvenile Western Ethiopian Shield during ca. 580–550 Ma. Importantly, the suture between them may represent the northern continuation of a major suture identified further south in Africa along which Gondwana amalgamated. Similarly, the Abas terrane in Yemen (Paper II) is dominated by reworking of pre–Neoproterozoic crust and shows age and isotopic compositions that are inconsistent with the Afif terrane of Saudi Arabia, precluding correlation between the two regions. The trace element systematics of plutonic rocks from the southernmost Arabian Shield (paper III) point to enrichment due to subduction component, bear no evidence of a plume component, and are consistent with the adakite-like chemistry of some of the subduction–related plutonic samples. This reinforces the notion that the shield grew through juvenile magmatic arc additions. The combined zircon U–Pb–O–Hf data of the Cambrian–Ordovician sandstones (Paper IV) indicate their derivation from both the adjacent juvenile ANS and the more southerly crustal blocks that are dominated by reworking of pre–Neoproterozoic crust. The remarkable similarity in age spectra and homogeneity of Cambrian sandstones deposited across the northern margin of Gondwana point to continental–scale sediment mixing and dispersal regulated by the supercontinent cycle.

Keywords: *Gondwana, Arabian–Nubian Shield, Azania, zircon U–Pb–O–Hf isotopes, Nd isotopes, Cambrian Sandstones, juvenile, pre–Neoproterozoic, reworking.*

Stockholm 2017
http://urn.kb.se/resolve?urn=urn:nbn:se:su:diva-145479

ISBN 978-91-7649-938-2
ISBN 978-91-7649-939-9

Department of Geological Sciences

Stockholm University, 106 91 Stockholm

CRUSTAL EVOLUTION OF THE ARABIAN–NUBIAN SHIELD

Fitsum Girum Yeshanew

Stockholm University

Crustal evolution of the Arabian–Nubian Shield

Insights from zircon geochronology and Nd–Hf–O isotopes

Fitsum Girum Yeshanew

ISBN print 978-91-7649-938-2
ISBN PDF 978-91-7649-939-9

Cover: Cambrian sandstone unconformably overlying Precambrian basement complex in Jordan
Printed in Sweden by Universitetsservice US-AB, Stockholm 2017
Distributor: Department of Geological Sciences

To Amelework, Girum and
my daughter, Johanna

ABSTRACT

The Arabian–Nubian Shield (ANS) represents a major site of juvenile Neoproterozoic crustal addition on Earth and documents Neoproterozoic tectonics bracketed by two supercontinent cycles, namely the fragmentation of Rodinia and the amalgamation of Gondwana. There is general consensus that the ANS formed by juvenile magmatic arc accretion and subsequent shield–wide post–tectonic magmatism. However, detailed understanding about the timing of events and the nature of magma sources in parts of the shield are lacking. To date, there are no isotopic data from the Paleozoic sedimentary sequences of the ANS, except those from the northern part. New zircon U–Pb, $\delta^{18}O$ and whole–rock Nd isotopes are presented for plutonic rocks from the eastern Ethiopia, Yemen and southernmost Arabian Shield in Saudi Arabia. This thesis also presents the first combined *in situ* zircon U–Pb–O–Hf isotope data on the Cambrian–Ordovician sandstones of the Arabian Shield. The results are used to elucidate the crustal evolution of these parts of the ANS and to evaluate terrane correlations. Specifically, the nature of crustal growth, i.e., relative proportions of juvenile magmatic additions vs. crustal reworking, nature of the magma source and mechanism of crust formation (plume material vs. subduction zone enrichment) and understanding the provenance of the Cambrian–Ordovician sandstone sequences were important research questions addressed.

The results from Paper I suggest that the eastern Ethiopian Precambrian basement is dominated by reworking of pre- Neoproterozoic supracrustal material unlike contemporaneous rocks in the remaining parts of Ethiopia—indicating the presence of two distinct lithospheric blocks of contrasting isotopic compositions in Ethiopia. Metamorphic age distributions suggest that the eastern Ethiopian block was amalgamated with the juvenile Western Ethiopian Shield during ca. 580– 550 Ma. Importantly, the suture between them may represent the northern continuation of a major suture identified further south in Africa along which Gondwana amalgamated. Similarly, the Abas terrane in Yemen (Paper II) is dominated by reworking of pre–Neoproterozoic crust and shows age and isotopic compositions that are inconsistent with the Afif terrane of Saudi Arabia, precluding correlation between the two regions. The trace element systematics of plutonic rocks from the southernmost Arabian Shield (paper III) point to enrichment due to subduction component, bear no evidence of a plume component, and are consistent with the adakite-like chemistry of some of the subduction–related plutonic samples. This reinforces the notion that the shield grew through juvenile magmatic arc additions. The combined zircon U–Pb– O–Hf data of the Cambrian–Ordovician sandstones (Paper IV) indicate their derivation from both the adjacent juvenile ANS and the more southerly crustal blocks that are dominated by reworking of pre–Neoproterozoic crust. The remarkable similarity in age spectra and homogeneity of Cambrian sandstones deposited across the northern margin of Gondwana point to continental–scale sediment mixing and dispersal regulated by the supercontinent cycle.

SAMMANFATTNING

I den Arabiska-Nubiska skölden (ANS) förekommer ett av de största och bäst blottade områdena på Jorden med juvenil Neoproterozoisk jordskorpa. Sköldområdet uppvisar Neoproterozoisk tektonik som begränsas i tid av två ”superkontinent-cykler”; nämligen fragmenteringen av Rodinia och amalgameringen av Gondwana. Det finns en konsensus om att ANS bildades genom tillväxt av juvenil magmatisk öbågeskorpa och efterföljande storskalig post-tektonisk magmatism. En detaljerad förståelse av tidsförloppen för olika geologiska händelser och karaktären för magmatismen i delar av skölden saknas emellertid. Till dags dato har det ej funnits isotopdata för Paleozoiska sedimentära bergartssekvenser inom ANS, med undantag för den norra delen. Nya data presenteras här för U-Pb och δ18O i zirkon och Nd isotoper i plutoniska bergarter från östra Etiopien, Yemen och från sydligaste delen av den Saudi-Arabiska skölden i Saudiarabien. I denna avhandling presenteras även den första studien med kombinerade, in-situ U–Pb–O–Hf isotopdata för zirkoner separerade från sandstenar av Kambrisk-Ordovicisk ålder från den Arabiska skölden. Resultaten har använts för att tolka den krustala utvecklingen av nämnda områden inom ANS och för att korrelera olika geologiska områden. Fokus har legat på att öka förståelsen av jordskorpans utveckling, och mer specifikt att kvantifiera andelen magmatiskt nybildad berggrund respektive den andel som representerar tektonisk omarbetning av äldre material, källan för magmatismen och mekanismer för krustal tillväxt (plym- versus subduktions-relaterad). En annan vital frågeställning har gällt provenansen för de undersökta sandstenarna av Kambrisk-Ordovicisk ålder.

Resultaten som återfinns i Uppsats I indikerar att basement i östliga Etiopien domineras av omarbetning av pre-Neoproterozoisk suprakrustalt material som skiljer sig från likåldrig berggrund i andra delar av Etiopen. Detta förhållande innebär att två distinkt olika berggrundsblock med skilda isotopsignaturer kännetecknar litosfären i Etiopien. Zirkonåldrar som tolkas motsvara metamorfa händelser implicerar att det östra etiopiska blocket amalgamerades med ett västligt block, som kännetecknas av juvenil berggrund, för ca 580-550 miljoner år sedan. Suturen mellan dessa block kan representera en nordlig förlängning av en mega-sutur längre söderut i Afrika som i sin tur definierar en zon utefter vars gräns amalgamering av Gondwana-kontinenten ägde rum. I likhet med ovan, är Abas-terrängen i Yemen (Uppsats II) dominerad av berggrund som utgör upparbetad äldre (pre-Neoprotrerozoisk) krusta. Denna terräng uppvisar en isotopsystematik och åldrar som icke är förenlig med Afif-terrängen i Saudi-Arabien, vilket innebär att dessa terränger inte kan korreleras på en geologisk basis. Spårelementsvariationer hos plutoniska bergarter från den allra sydligaste delen av den Arabiska skölden (uppsats III) tolkas som att en anrikning skett genom påverkan av en subduktionskomponent. Spårelementsystematiken visar inga tecken på något inflytande av en plym-komponent och detta stöds också av en adakit-lik kemi för några av de subduktionsrelaterade plutoniterna. Detta förhållande understryker att skölden tillväxte genom additioner av juvenilt öbågerelaterat material. Kambrisk-Ordoviciska sandstenar har undersökts med olika metoder (uppsats IV) och kombinerade U-Pb-O-Hf isotopdata är förenligt med att utgångsmaterialet till dessa bergarter kom dels ifrån närliggande juvenil ANS berggrund liksom från krustala block, som återfinns längre söderut, vilka är dominerade av omarbetat äldre (pre-Neoproterozoiskt) material. Det finns en remarkabel likhet hos Kambriska sandstenar både vad gäller ålderspektra och homogenitet tvärs över de nordliga delarna av Gondwana. Detta kan tas som en indikation på att det förekommit en storskalig blandning och transport av sediment som en del av en ”superkontinent-cykel”.

List of papers

This doctoral thesis consists of a summary and four papers listed below as Papers I–IV. Papers I and II are reprinted with permissions from The Geological Society of London and Elsevier, respectively.

Paper I: **Yeshanew, F. G**., Pease, V., Abdelsalam, M. G., Whitehouse, M. J., 2017. Zircon U–Pb ages, δ18O and whole-rock Nd isotopic compositions of the Dire Dawa Precambrian basement, Eastern Ethiopia: Implications for the assembly of Gondwana. Journal of the Geological Society, London. 174, 142–156. doi:10.1144/jgs2016-017

Paper II: **Yeshanew, F. G**., Pease, V., Whitehouse, M. J., Al-Khirbash, S., 2015. Zircon U-Pb geochronology and Nd isotope systematics of the Abas terrane, Yemen: Implications for Neoproterozoic crust reworking events. Precambrian Research. 267, 106–120. doi:10.1016/j.precamres.2015.05.037

Paper III: **Yeshanew, F. G**., Pease, V., Whitehouse, M. J. Magmatic evolution of the southernmost Arabian shield inferred from integrated zircon U-Pb ages, whole-rock geochemistry, and Nd isotopes, Manuscript.

Paper IV: **Yeshanew, F. G**., Whitehouse, M. J., Pease, V., Daly, S. Continental–scale sediment mixing and dispersal across northern Gondwana: Evidence from detrital zircon U–Pb–O–Hf isotope systematics of the Cambrian–Ordovician sandstones of the Arabian Shield, Manuscript.

Paper I: F. G. Y. made all the analyses and wrote the manuscript. M. G. A. collected the samples and wrote most of the ‘‘Geological setting and previous work’’ section. All co-authors commented on the manuscript.

Paper II: F. G. Y. made all the zircon U–Pb and part of the Sm–Nd analyses and wrote the manuscript. S. A. K. collected the samples and made the whole–rock geochemical and part of the Sm–Nd analyses. All co-authors contributed in the revision of the manuscript.

Paper III: F. G. Y. and V. P. collected the samples. F. G. Y. made all the analyses and wrote the manuscript. All co-authors commented on the manuscript and contributed in terms of text revision and scientific discussions.

Paper IV: F. G. Y. and M. J. W. collected the samples. F. G. Y. did all the zircon U–Pb–O analyses and M. J. W. did the Lu–Hf analyses and assisted in subsequent data interpretation. F. G. Y. wrote the manuscript and all co-authors took part in revisions and pertinent scientific discussions.

CONTENTS

1. INTRODUCTION

1.1. The continental crust

The continental crust has an average andesitic composition and is buoyant because of its lower density compared to the underlying mantle, resulting in its preservation over geological time. The presence of the continental crust on Earth is one of the main features that distinguish it from other terrestrial planets in the Solar System (Campbell and Taylor, 1983; Rudnick, 1995). The contrasting compositional and mechanical properties of the oceanic and continental crust are the manifestations of plate tectonics on Earth and how the planet dissipates heat (Condie, 2011). The vertical extent of both the continental and oceanic crust is defined by a jump in primary seismic waves (>7.6 kms^{-1}) and is known as the Mohorovičić discontinuity. This seismically defined crust–mantle boundary is not always the same as the compositional crust–mantle boundary (Griffin and O'Reilly, 1987). The ocean–continent transition marks the lateral extent of the continental crust (Cogley, 1984; Levander et al., 2006). The thickness of the continental crust varies between 30 and 80 km, averaging ~39 km (Christensen and Mooney, 1995). The thickness can be greatly attenuated in regions of active continental rifting, e.g., the Afar Rift System, part of the Main Ethiopian Rift, is only 16 km thick (Hayward and Ebinger, 1996).

1.2. Evolution of the continental crust

Fundamentally different modes of convection occur among planets in the Solar System. While plate tectonics is known to occur only on Earth, 'stagnant lid' convection prevails in neighboring planets Venus and Mars (Schubert et al., 2001; Breuer and Spohn, 2003) and may also have characterized the earliest Earth (e.g. Kamber et al., 2005). The negative buoyancy of cold and dense oceanic lithosphere primarily drives modern–style plate tectonics on Earth via slab-pull mechanisms (Molnar and Atwater, 1978; Patriat and Achache, 1984). Plate tectonic processes are the direct consequence of mantle convection, which is strongly dependent upon viscosity and by implication mantle temperature (van Hunen et al., 2008). Subduction zones are the major sites of crustal growth and other tectonic settings such as continental rifts and hot spots are less important (Stern, 2010; Taylor and McLennan, 1995). However, some authors (e.g., Stein and Goldstein, 1996; Stein and Hofmann, 1994) attribute a significant role to mantle plumes in the generation of the continental crust in the past. Our understanding of the development and evolution of plate tectonics on Earth influences how we view the history and dynamics of extraterrestrial planets and their habitability (Kasting and Catling, 2003; Korenaga, 2013). Despite consensus that the prime mechanism driving the evolution of the Earth system and planetary habitability is plate tectonics, when and how it began is a matter of considerable debate (e.g., Condie and Pease, 2008). Consensus is lacking regarding when plate tectonics on Earth began, with suggestions spanning almost the entire Earth's history. These diverging views partly stem from the varying emphasis placed upon different criteria to recognize the operation of plate tectonics. For instance, Stern (2008, 2005) proposed modern-style plate tectonics began in the Neoproterozoic. The evidence put forward in support of this claim is the lack of high-pressure metamorphic rocks and ophiolites of pre-Neoproterozoic age (Stern, 2005). On the other hand, some authors (e.g., Harrison et al., 2008; Hopkins et al., 2008) suggest that plate tectonics began in the Hadean (> 4.0 Ga). These very early estimates for the onset of plate tectonics are mainly based on the oxygen isotope signatures and geochemistry of Hadean zircons, and mineral inclusions in these zircons, which suggest they may be derived from evolved continental crust (Mojzsis et al., 2001; Wilde et al., 2001). The majority of authors, however, suggest that plate tectonics began in the Archean (Brown, 2006; Condie et al., 2008; Kranendonk et al., 2007; Shirey et al., 2008; Tang et al., 2016).

The origin, rate and mechanism of crust formation are fundamental questions in the earth sciences. Various models have been proposed for the rate of continental growth through time and are mostly based on geochronological and isotopic data from

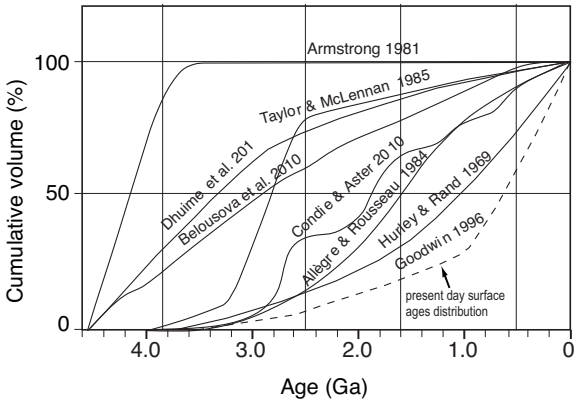

Figure 1. Crustal growth curves through time from the Haden to the present. Modified from Cawood et al. (2013).

rocks and minerals. Early models (Hurley and Rand, 1969) proposed a linearly increasing continental crustal growth rate from ca. 3.1 Ga (Fig. 1). This

model is mainly based on whole-rock Rb-Sr and K-Ar geochronological data (Hurley, 1968; Hurley and Rand, 1969); we now know, however, that the lower closure temperatures of these isotopic systems makes them susceptible to isotopic homogenization or disturbance during later tectonothermal events that may bias them towards younger ages (e.g., Cawood et al., 2013). A second model proposes a surge in the rate of continental growth earlier in earth history followed by steady-state growth (Armstrong, 1981; Fyfe, 1978; Fig. 1). Other models (e.g., Belousova et al., 2010; Dhuime et al., 2012; Fig. 1) infer continuous growth of the continental crust with a rapid rate in the Archean.

Sediments are good natural samplers of the extant continental crust at the time of erosion and sedimentation. It is possible that, especially for Precambrian terranes, plutons have either been fully eroded (erased) from the geological record or are buried under younger sediments, and that sediment detritus is their only vestige. A good example is the Jack Hills metasedimentary sequence, which contain zircons as old as ca. 4.4 Ga (Wilde et al., 2001) yet rocks older than the Acasta gneiss (ca. 4.03 Ga) are unknown globally (Bowring and Williams, 1999). The ages of orogenic granites and detrital zircon through time, as well as other geological proxies, show uneven distributions with peaks and troughs (Campbell and Allen, 2008; Condie, 1998; Condie et al., 2009; Hawkesworth and Kemp, 2006; Iizuka et al., 2013; Kemp et al., 2006; this thesis). The peaks in zircon U-Pb ages (Fig. 2) broadly correlate with the time of supercontinent assembly (Campbell and Allen, 2008). Other geological proxies such as the abundance of passive margins, seawater $^{87}Sr/^{86}Sr$ ratios and high-grade metamorphism also show fluctuations which appear to be controlled by supercontinent cyclicity (Bradley, 2011; Brown, 2007; Veizer and Mackenzie, 2014). For instance, the abundance of Phanerozoic passive margins shows fluctuations that coincide with the assembly, tenure and dispersal of the supercontinent Pangea, and similar patterns are observed for Precambrian passive margins as well (Bradley, 2011). The secular trends in zircon crystallization ages have been interpreted in two fundamentally different ways. Some authors relate the peaks in ages to major short–lived episodes of juvenile crust formation associated with enhanced mantle plume activity (Albarède, 1998; Arndt, 2013; Condie, 1998; Reymer and Schubert, 1986; Stein and Goldstein, 1996; Stein and Hofmann, 1994). Such pulses of accelerated crustal growth have been interpreted to result from superplume events caused by a descending slab(s) catastrophically sinking to the base of the upper mantle (Condie, 1998) or to mantle overturn and penetrative convection triggered by a descending slab(s), both of which result in rapid and extensive crust generation through accretion of plume heads (Stein and Hofmann, 1994). In this episodic crust generation model, age gaps in the zircon age spectra are interpreted to represent quiescent periods of low crust–formation during two–layer mantle convection cycles and crustal growth via arc accretion (Stein and Hofmann, 1994) or in some cases to be due to a cessation of magmatism (Condie et al., 2009b). Another model links the peaks in the age spectra to supercontinent cyclicity (Campbell and Allen, 2008; Condie et al., 2011; Condie and Aster, 2010; Gurnis and Davies, 1986; Hawkesworth et al., 2009, 2010; Lancaster et al., 2011). As we go further back in time, the uncertainty on the timing of supercontinent assembly, tenure and dispersal becomes larger, and relating the zircon crystallization age peaks to supercontinent assembly is less straightforward (Arndt, 2013).

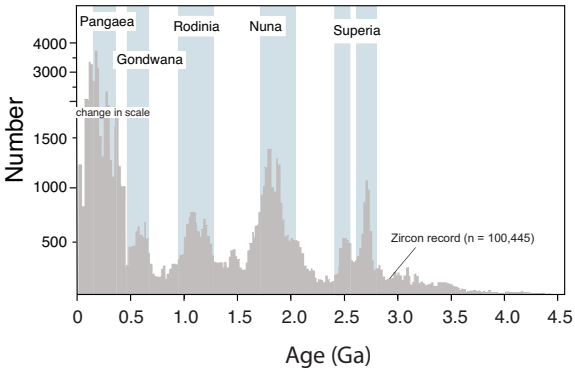

Figure 2. Global detrital zircon distribution (n > 100, 000; ≥ 95% concordant analyses) and times of supercontinent formation throughout Earth history. Redrawn from Cawood et al. (2013) with data from Voice et al. (2011).

2. GEOLOGICAL BACKGROUND

The late Neoproterozoic to early Cambrian assembly of Gondwana along the East African Orogen (EAO) (Stern, 1994) resulted in one of the largest mountain belts in Earth's history (Squire et al., 2006). The assembly of Gondwana coincided with dramatic changes in ocean chemistry (e.g., the increase in the $^{87}Sr/^{86}Sr$ isotopic excursion), a surge in atmospheric oxygen, a major oxygenation of the deep oceans, 'snowball' glaciations and the emergence and expansion of animals (Bradley, 2011; Campbell and Squire, 2010; Canfield et al., 2007; Fike et al., 2006; Squire et al., 2006). The higher erosion rates of the 'Transgondwanan supermountains', formed in the aftermath of Gondwana amalgamation, are thought

to have enhanced photosynthetic O_2 production (Campbell and Allen, 2008; Campbell and Squire, 2010). Thus, the implication is that the formation of Gondwana controlled ocean chemistry, oxygenation events and erosion at the end of the Neoproterozoic. Therefore, understanding the detailed chronology of events and deciphering the origin of Neoproterozoic crustal segments such as the Arabian–Nubian Shield (ANS) contributes to our understanding of this important period in Earth's history.

About a fifth of the exposed continental crust is estimated to be Neoproterozoic in age or reworked during this time (Stern, 2008b). Neoproterozoic crust formation is likely to be more important than yet considered. Stern (2008b) identified the following possible reasons as to why Neoproterozoic crustal growth could be more important than appreciated: (1) Most Neoproterozoic crust and the now dispersed the parts of the supercontinent Gondwana occur in regions that lack detailed studies related to crustal evolution; (2) The Neoproterozoic lithospheric mantle is generally denser than the lithosphere of older cratons, thus Neoproterozoic crust is often covered by younger sediments due to isostatic readjustment; and (3) In some regions, Neoproterozoic crust is masked by younger tectonomagmatic events, so understanding its true extent requires detailed geochronological and isotopic investigations.

The Arabian–Nubian Shield (Figure 3) represents a protracted accretion of juvenile arc terranes with anomalously high rate of juvenile magmatic addition (Duyverman et al., 1982; Johnson and Woldehaimanot, 2003; Patchett and Chase, 2002; Reymer and Schubert, 1984; Stern, 1994). Until Tertiary time, the shield was blanketed by a thick Paleozoic sequence. Rifting of the Red Sea accompanied by regional uplift exposed the Neoproterozoic crystalline basement of the ANS on its flanks (Cooper et al., 1979). The ANS dominantly formed through magmatic arc addition within the Mozambique Ocean (Fleck et al., 1980; Stern, 1994; Stoeser and Frost, 2006). Abundant Neoproterozoic ophiolites (ca. 870–690 Ma) in the ANS are consistent with a convergent margin setting (Berhe, 1990; Stern et al., 2004). The evolutionary history of the ANS is intimately linked with Neoproterozoic supercontinent cycles (Stern, 1994; Stern and Johnson, 2010) and the northern sector of the East African Orogen underwent a series of orogenic events bracketed by the fragmentation of Rodinia (ca. 879 Ma) and the assembly of Gondwana (ca. 550 Ma) (Jacobs and Thomas, 2004; Johnson and Woldehaimanot, 2003; Li et al., 2008; Stern, 1994; Yeshanew et al., 2017). The ANS is therefore an ideal place to study Neoproterozoic plate tectonics and crust forming processes, as well as Neoproterozoic development of oceans, weathering, seawater compositions and atmosphere development (Pease and Johnson, 2013; Stern et al., 2013).

The Neoproterozoic age and juvenile nature of the ANS is well-known from geochronological and radiogenic isotopic studies (Be'eri-Shlevin et al., 2010; Duyverman et al., 1982; Fleck et al., 1980; Hargrove et al., 2006; Stern, 2002, 1994; Stoeser and Frost, 2006). Xenolith investigations, such as those from the Cenozoic basalts (Mcguire and Stern, 1993; Stern et al., 2016; Stern and Johnson, 2010), indicate the juvenile character of the lower crust and lithospheric mantle of the ANS which likely formed concurrently with its upper crust (Stern and Johnson, 2010). However, reworked pre-Neoproterozoic crustal fragments are recognized at the ANS margins. These pre–Neoproterozoic crustal fragments include the isotopically delineated Khida sub–terrane in eastern Saudi Arabia (Fig. 4; Agar et al., 1992; Stacey and Agar, 1985; Whitehouse et al., 2001), the arc–gneiss collages of the Precambrian basement of Yemen (Whitehouse et al., 2001; Windley et al., 1996; Yeshanew et al., 2015) and the eastern Ethiopian–northwestern Somalian crustal block (Fig. 3; Kröner and Sassi, 1996; Teklay et al., 1998; Yeshanew et al., 2017). Based on zircon inheritance patterns, Hargrove et al. (2006) suggested that about a third of the juvenile core of the ANS was contaminated by continental material. The Sa'al metamorphic complex in Sinai yielded crystallization ages of ca. 1.0–1.1 Ga with minor Paleoproterozoic and Archean inherited zircons (Be'eri-Shlevin et al., 2012; Be'eri-Shlevin et al., 2009). These authors interpreted the late Mesoproterozoic crystallization ages to indicate the presence of Mesoproterozoic crust in the northernmost ANS. A comprehensive compilation of zircon inheritance in the ANS indicates that about 5% of dated zircons have ages that predate the earliest tectonomagmatic events in the ANS (Stern et al., 2010). Furthermore, there is a systematic variation in zircon inheritance patterns in the ANS with mafic rocks preserving more inherited zircons than alkali-rich felsic ones, and the abundance of inherited zircons in volcanic rocks is four times their plutonic counterparts (Stern et al., 2010). Interestingly, the demonstrably pre-Neoproterozoic Abas terrane (highly evolved $\varepsilon_{Nd}(t)$) yielded few inherited zircons (Yeshanew et al., 2015). This study highlights that the mere presence or absence of inherited zircons alone is not a reliable indicator of the true nature of the source rocks, as the preservation of zircon is highly dependent upon magma temperature

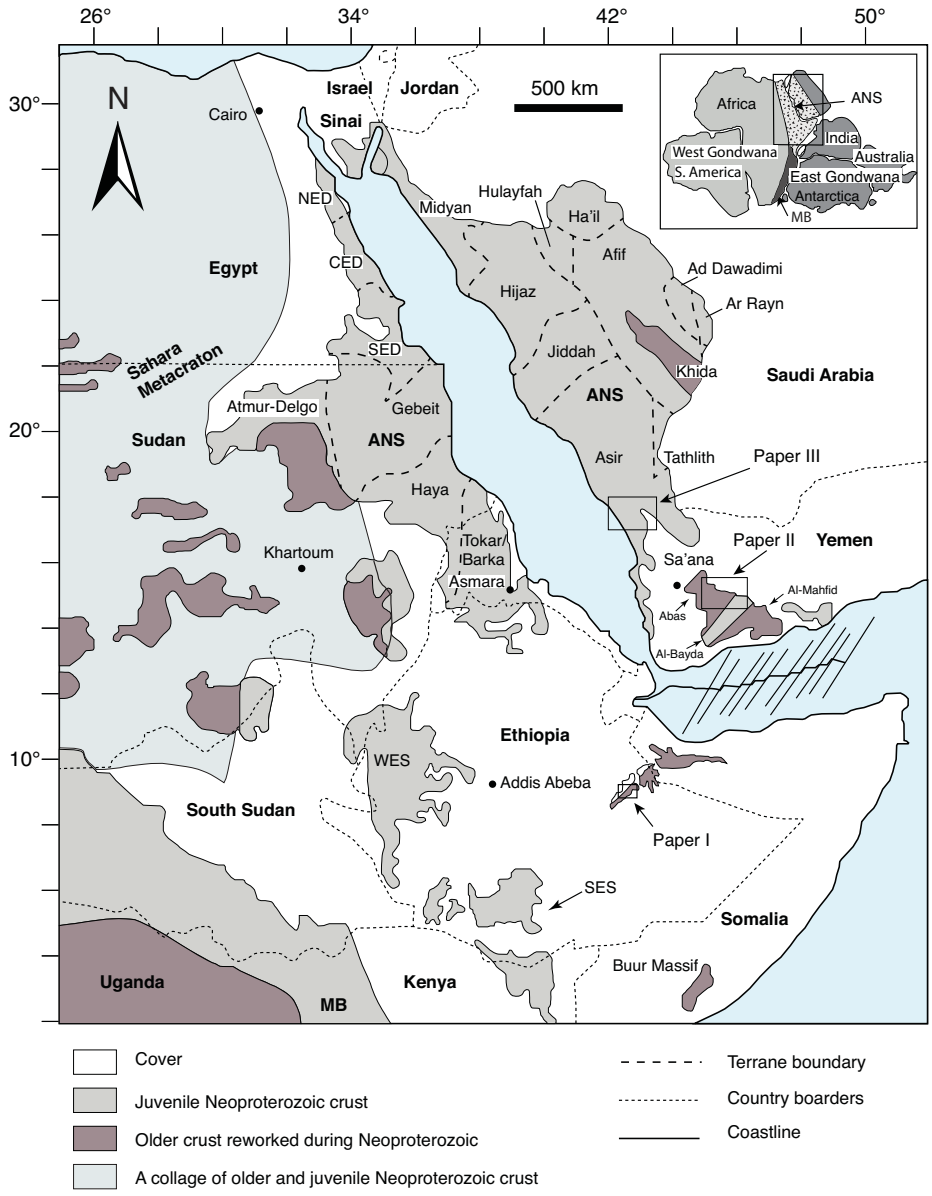

Figure 3. Precambrian exposures of the Arabian–Nubian Shield (modified after Worku and Schandelmeier, 1996; Fritz et al., 2013; Blades et al., 2015) with locations of the plutonic samples (Papers I–III) labelled. The Gulf of Aden fracture patterns are drawn from Bosworth et al. (2005). Inset shows the East African orogen consisting of the Arabian–Nubian Shield and the Mozambique Belt (after Abdelsalam et al., 2008). WES, Western Ethiopian Shield; SES, Southern Ethiopian Shield; NED, Northern Eastern Desert; CED, Central Eastern Desert: SED, Southern Eastern Desert.

and composition (Watson and Harrison, 1983).

The Najd Fault System (NFS) is a strike–slip fault zone and a principal structure in the Arabian Shield that post–dates its cratonization (Fig. 4; Agar, 1987; Stern, 1985). Although displacement across the NFS is dominantly sinistral along NW–SE trending branches, local dextral movement has also been postulated/noted in some parts of the NFS, particularly across its NNE–SSW trending branches (Agar, 1987; Kusky and Matsah, 2003). The occurrence of 'syntectonic' plutons within the NFS may suggest a causal link between Najd deformation and magmatism (Johnson et al., 2011; Stern, 1985). The NFS also played a role in the exhumation of deep crustal gneiss domes and locally altered crustal rheology (Johnson et al., 2011; Meyer et al., 2014).

The age, isotopic character, stratigraphy and structure of the Arabian Shield island arc assemblages allows them to be divided into eight distinct tectonostratigraphic terranes with their boundaries marked by ophiolite–bearing suture zones (Fig. 4b; Johnson et al., 2011; Johnson and Woldehaimanot, 2003; Stoeser and Frost, 2006). These island arc terranes form two structural entities: the western arc terranes consisting of the Midyan, Hijaz, Asir and

Jiddah terranes and the eastern arc terranes consisting of the Ha'il, Afif, Tathlith, Ad Dawadimi and Ar Rayn terranes (Stoeser and Frost, 2006). Earlier amalgamated groups of the western island arc terranes collided with their eastern counterparts along the N–S trending, serpentinite–decorated Nabitah Mobile Belt (NMB) (Fig. 4b; Johnson et al., 2011; Johnson and Woldehaimanot, 2003; Pallister et al., 1987; Quick, 1991; Stoeser and Camp, 1985). The NMB was affected by dextral shear throughout its history (Johnson and Woldehaimanot, 2003). The amalgamation of the shield along the NMB was accompanied by magmatic, deformational and metamorphic events collectively known as the Nabitah orogen (Johnson et al., 2011). Zircon U–Pb ages of synorogenic plutons within the NMB, particularly in its southern segment, indicate that deformation was active during ca. 680–640 Ma (Stoeser et al., 1985; Stoeser and Camp, 1985). This earlier model ascribes the NMB a significant a role in the accretionary and collisional history of the Arabian Shield, however, recent studies have revised its role in the evolution of the shield. For instance, a geochronological and isotopic study of samples collected across the NMB from the Asir composite terrane shows isotopic similarities across the NMB and implies that it is an intra oceanic arc suture, thus the major suture between the western oceanic arc and eastern oceanic arc–continental block terranes must lie to the east of the NMB (Flowerdew et al., 2013).

The protracted (ca. 300 Ma) tectonomagmatic evolution of the shield is commonly divided into four tectonomagmatic stages, each characterized by magma generation and emplacement of plutonic rocks: (1) The oldest assemblages of oceanic basalt mainly exposed in the western Arabian Shield (Fleck et al., 1980), (2) formation and amalgamation of intra–oceanic island arc complexes during ca. 900–650 Ma (Bentor, 1985; Fleck et al., 1980, 1976), (3) brief (ca. 50–60 Ma) but extensive emplacement of post–tectonic calc-alkaline batholiths characterized by more differentiated magmas from ca. 640–570 Ma throughout the shield (Ali et al., 2009; Be'eri-

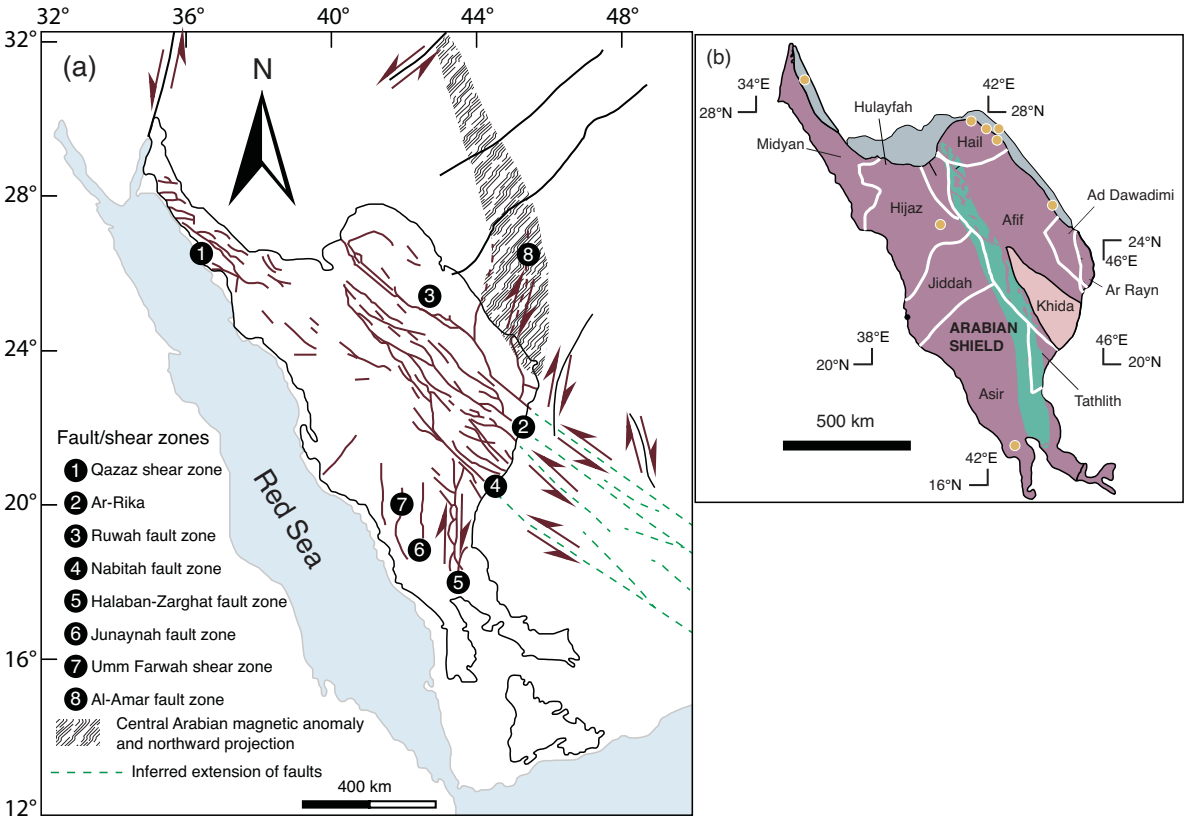

Figure 4. (a) Geological map of the Arabian Shield depicting prominent Precambrian faults within the shield (modified from Stern and Johnson, 2010); Johnson et al., 2011) and (b) map showing the individual terranes, the Nabitah shear zone and the Cambrian–Ordovician sandstone exposures (shaded grey). Sample locations of the sandstones (Paper IV) are marked with orange circles.

Shlevin et al., 2009; Bentor, 1985; Cooper et al., 1979; Eyal et al., 2010; Fleck et al., 1980; Yeshanew et al., 2015), and (4) alkaline–peralkaline magmatism at ca. 600 Ma in an extensional setting suggesting the end of orogenesis (Be'eri-Shlevin et al., 2009; Bentor, 1985; Eyal et al., 2010; Stern, 1994; Yeshanew et al., 2015). Although the above evolutionary scheme for the evolution of the ANS is generally accepted, the nature of magmatic source regions, mechanisms of magma generation, and the timing of transitions between these phases are debated.

The most extensive phase in the ANS magmatic history is the island-arc stage, which lasted for about 200 Ma, comparable to the lifespan of arc magmatism in western Pacific (Fleck et al., 1980; Stein, 2003). The arc rocks are mostly calc–alkaline but in some cases tholeiitic and encompass a wide spectrum of rock types such as basalts, boninites, andesites, rhyolites, volcanosedimentary rocks, abundant tonalite–trondhjemite–granodiorite (TTG) suites Volumetrically, there is an inverse relationship between the abundance of island arc intrusive rocks (Stage II) and the post-tectonic batholiths (Stage III) between the northern and southern ANS. Post-tectonic granitoids are predominant in the northern ANS and are least abundant in the southwestern Arabian Shield (Bentor, 1985; Fleck et al., 1980; Stern and Hedge, 1985), while the inverse is true for the magmatic arc rocks of the shield. The volcanic rocks of the post–tectonic stage, also calc-alkaline in composition (Stage III), have a geographic bias like their plutonic equivalents. They are most abundant in the Sinai Peninsula of the northern ANS and in the Eastern Desert of Egypt, and are essentially absent in the central and southern Arabian Shield of Saudi Arabia (Bentor, 1985). High-spatial resolution SIMS zircon dating of post-tectonic granitoids demonstrated that the calc-alkaline and alkaline suites temporally overlap; in the northernmost ANS and in the Precambrian basement of Yemen the two suites are contemporaneous at ca. 605 Ma, indicating a gradual transition from calc-alkaline to alkaline (Be'eri-Shlevin et al., 2009; Yeshanew et al., 2015). Calc-alkaline and alkaline post–tectonic rocks emplaced at ca. 625–600 Ma are interpreted to result from delamnation or slab roll-back/tear (Avigad and Gvirtzman, 2009; Flowerdew et al., 2013).

3. OBJECTIVES OF THE THESIS

The ANS has a protracted history with its early stage characterized by arc magmatism (Stern, 1994; Johnson and Woldehaimanot, 2003), although plume magmatism may also be involved (Stein, 2003; Stein and Goldstein, 1996; Teklay et al., 2002). Late-stage ANS evolution is characterized by voluminous emplacement of post–tectonic calc-alkaline and alkaline batholiths (Bentor, 1985; Be'eri-Shlevin et al., 2009). Identifying juvenile vs. reworked crust and associated mechanisms (arc vs. plume material) has implications for the rate of crustal growth in the ANS. The late-stage post-tectonic calc-alkaline and alkaline plutons also provide insights into the final stages of the shield's evolution during the assembly of the supercontinent Gondwana. This thesis seeks to better understand the crustal evolution of the ANS, including the southernmost Arabian Shield and the Precambrian arc–gneiss collage in Yemen and eastern Ethiopia. These parts of the ANS generally lack systematic geochronological and isotopic study. Evaluation of terrane correlations both within the Arabian Peninsula and across the Gulf of Aden between the Precambrian basement of northeast Africa and Arabia is also an important facet of this thesis. Towards these goals, the thesis has two principal components:

Component 1: Plutonic rocks were sampled from the Asir terrane, southernmost Arabian Shield, from the Abas terrane in Yemen, and from the Dire Dawa Precambrian basement in eastern Ethiopia (Fig. 3). Samples span a wide range of magmatic affinities that temporally span from the earliest arc-related to post-tectonic alkaline plutons that herald the end of orogenesis in the region. Secondary ion mass spectrometry (SIMS) U-Th-Pb geochronology and ^{18}O and whole-rock Nd isotopic and geochemical data evaluate the relative contributions of juvenile vs. reworked crust and track the evolution of the ANS from island arc to cratonization.

Component 2: The assembly of Gondwana and the mountain belts that formed during collisional orogenesis can be traced through analyses of the sedimentary rocks derived from them (Squire et al., 2006). The detrital sedimentary record effectively samples large areas and ranges of source rocks of the extant continental crust at the time of sedimention (Cawood et al., 2013). In the aftermath of Gondwana assembly, voluminous clastic sediments were deposited on a vast, continental–scale, peneplain on the northern margin of Gondwana including the ANS (Burke et al., 2003). Cambrian–Ordovician sandstone samples collected across ca. 1600 km, from southern Jordan and the Arabian Shield in Saudi Arabia provide excellent spatial coverage and allow geographic variations in provenance to be evaluated. SIMS U–Pb dating of zircons from these sandstone samples

provide age control while O- and Hf-isotopic analyses enable the magmatic history and source reservoir information to be decrypted. Paleocurrent studies indicate that the sediments were transported from the south (Dabbagh and Rogers, 1983) and, combined with the zircon U-Pb, O, and Hf analyses, will provide unique insight into the role of juvenile crustal growth vs. reworking in the hinterland of Gondwana.

4. METHODS

4.1. Zircon

Zircon ($ZiSiO_4$) is a ubiquitous accessory phase in evolved magmatic rocks but also occurs in mafic rocks at very low abundance. Zircon growth has also been documented during medium-to high-grade metamorphism (Whitehouse and Platt, 2003; Harley et al., 2007). Whether zircon has a magmatic or metamorphic origin can be deciphered through imaging and chemical analyses (Corfu et al., 2003; Hoskin and Schaltegger, 2003; Whitehouse et al., 1999). Zircon's physical resilience and chemical inertness makes it an ideal chronometer and tracer mineral for studies ranging from the early earth dynamics to recent orogenic processes. Zircon hosts trace elements whose isotopic pairs are of great importance in geochronology and isotope geochemistry. These include the U-Th-Pb and the low-temperature U-Th/He chronometers, stable O isotopes and the ^{176}Lu-^{176}Hf isotope system, which is a powerful tool to understand crust-mantle differentiation events.

4.2. Sample preparation

The separation and purification of zircon from whole-rock samples require care to avoid contamination. Heavy mineral fractions are obtained from crushed, milled and sieved rock samples using a hydrodynamic separation method utilizing a Wilfley table. Mineral fraction can be further purified using magnetic separation since minerals of different compositions have different magnetic susceptibilities. Sorting of zircons through magnetic separation and selection of the least paramagnetic ones has been shown to improve the concordance of ages (Krogh, 1982). Other methods, not used in this thesis, that were found to remove metamict (radiation–damaged) portions and hence improve concordance include mechanical abrasion (Goldich and Fischer, 1986; Krogh, 1982) and thermal annealing and partial–dissolution (Ramezani et al., 2007).

After purification, zircon is hand-picked and sorted according to morphology, color and size under the binocular microscope and mounted into double-sided tape; epoxy is then poured onto the zircon grains using a mould. The epoxy mounts are then polished to expose any inherited zircons or internal structures of the zircons. Proper polishing of sample mounts is of paramount importance in secondary ion mass spectrometry (SIMS) analyses. The degree of polishing relief correlates with the reproducibility of e.g. SIMS oxygen isotope analyses, with sample topography of ca. 10 µm resulting in a ca. 2‰ analytical artefact (Kita et al., 2011, 2009). This is because the sample relief distorts the equipotential surface and therefore the path of the secondary ion trajectory, which in turn affects the measured isotope ratios (Kita et al., 2009). This correlation of sample relief and reproducibility emphasizes the importance of sample polishing prior to SIMS analyses. Polished mounts are then gold–coated to avoid charging during the sputtering process and to enhance extraction of the secondary ions (Hinthorne et al., 1979; Hinton and Long, 1979; Ireland and Williams, 2003a).

Zircon often displays magmatic growth zones that reflect evolving melt compositions, incorporation of grains that pre-date the main magmatic event (inheritance) or post-crystallization processes (Corfu et al., 2003). Various imaging techniques such as optical microscopy, back–scattered electron and cathodoluminescence are routinely employed to document such intra–grain complexities prior to SIMS analyses (e.g., Whitehouse et al., 1999). Such studies have shown that zircon can have internal structure far more complex than previously realized. Therefore, image analysis is an essential aspect of *in-situ* high–spatial resolution SIMS zircon isotope analyses and enables one to choose discrete growth zones within a single grain and avoid inclusions, cracks or radiation damaged zones which could result in problematic data (Hanchar and Miller, 1993; Nemchin et al., 2013).

4.3. Zircon U–Pb geochronology

The crystal structure of zircon allows modest amounts of U and Th but Pb is fairly unwelcome. The radiogenic ingrowth of Pb isotopes from the decay of their respective parent U and Th isotopes enables accurate and precise age determinations. Under most magmatic conditions, diffusion of elements these parent–daughter pairs is very low (Cherniak and Watson, 2000). By the fluke of nature, two chemically identical uranium isotopes, ^{235}U and ^{238}U independently decay at different rates to their respective radiogenic daughter isotopes of ^{207}Pb and ^{206}Pb, making this dual

decay scheme unique among all radioactive dating systems (Parrish and Noble, 2003; Williams, 1998). Pb has four naturally occurring isotopes: ^{204}Pb, ^{206}Pb, ^{207}Pb and ^{208}Pb. Among these only ^{204}Pb is non-radiogenic and ^{208}Pb is the decay product of ^{232}Th. The decay of ^{232}Th, ^{235}Uand ^{238}U involve several short–lived intermediate isotopes. The decay schemes for the two uranium isotopes can be expressed as follows: (Fig. 5)

$$\left(\frac{^{206}Pb}{^{204}Pb}\right) = \left(\frac{^{206}Pb}{^{204}Pb}\right)_i + \left(\frac{^{238}U}{^{204}Pb}\right)\left(e^{\lambda_{238}t} - 1\right) \quad [1]$$

$$\left(\frac{^{207}Pb}{^{204}Pb}\right) = \left(\frac{^{207}Pb}{^{204}Pb}\right)_i + \left(\frac{^{235}U}{^{204}Pb}\right)\left(e^{\lambda_{235}t} - 1\right) \quad [2]$$

Where λ^{235} and λ^{238} are decay constants of ^{235}U and ^{238}U with values of 1.55125×10^{-10}y^{-1} and 9.8485×10^{-10} y^{-1} (Steiger and Jäger, 1977). Compared to the final decay chain, the intermediate steps are very short–lived and can be omitted and the isochron equations can be reduced to relate only the ultimate parent atoms remaining in the system to the final radiogenic daughter atoms as follows:

$$\frac{^{206}Pb^*}{^{238}U} = e^{\lambda_{238}t} - 1 \quad [3]$$

$$\frac{^{207}Pb^*}{^{235}U} = e^{\lambda_{235}t} - 1 \quad [4]$$

The asterisk represents radiogenic ingrowth of daughter isotopes accumulated as a result of the decay of their parent isotopes. If the ages from these two independent decay schemes, calculated using their respective decay constants and the measured ^{206}Pb*/^{238}U and ^{207}Pb*/^{235}U, are identical, the age is called concordant, indicating a closed isotopic system (Ahrens, 1955; Wetherill, 1963, 1956). If the ages obtained are different, the age is termed discordant and signifies isotopic disturbance. The curve fitted through an infinite number of concordant points, constructed using equations [3] and [4], is called a concordia curve (Fig. 5). The two most common causes of discordance are sampling of mixed growth zones, i.e.- older and younger growth zones, and post–crystallization Pb–loss due to later tectonothermal events.

U–Pb data is presented in various ways, but the Wetherill (or Conventional) and the Tera–Wasserburg (or Inverse) concordia diagrams are the most widely used (Fig. 5). Such diagrams enable data visualization and features such as Pb–loss can easily be discerned. The Wetherill concordia diagram (Wetherill, 1963, 1956) is constructed by plotting ^{207}Pb*/^{235}U vs. ^{206}*/^{238}U. This (Wetherill) concordia diagram relies on the radiogenic daughter isotopes, so its application to systems that incorporate excess radiogenic daughter isotopes is problematic. For instance, in the early 1970s Lunar samples yielded ages older than those determined using other dating systems and this was attributed to excess radiogenic Pb isotopes incorporated at the time of crystallization (Tatsumoto, 1970; Tera and Wasserburg, 1972). To circumvent this problem, Tera and Wasserburg (1972) came up with the inverse concordia diagram, also known as the Tera–Wasserburg concordia diagram, that plots ^{238}U/^{206}Pb vs. ^{207}Pb/^{206}Pb and has the benefit of easily distinguishing modern and ancient Pb-loss.

4.4. Zircon δ^{18}O

Oxygen (O) has three naturally occurring stable isotopes: ^{16}O, ^{17}O and ^{18}O with abundances of 99.762%, 0.038% and 0.200%, respectively (Faure and Mensing, 2005). Because of large differences in mass between the heaviest and the lightest O isotopes, they are subject to mass-dependent fractionation (Hoefs, 2004). The ratio ^{18}O/^{16}O is determined for geological applications since these two O isotopes have greater abundances and mass difference (Hoefs, 2004). The ^{17}O/^{16}O has important cosmological application (McSween and Huss, 2010). The ratio ^{18}O/^{16}O is expressed relative to the Standard Mean Ocean Water (SMOW) and is designated as δ^{18}O. The ratio δ^{18}O is expressed as follows:

$$\delta^{18}O = \left[\frac{\left(\frac{^{18}O}{^{16}O}\right)_{Sample}}{\left(\frac{^{18}O}{^{16}O}\right)_{SMOW}} - 1\right] \times 10^3 \quad [5]$$

Zircon has a very slow oxygen diffusion rate and therefore preserves magmatic δ^{18}O unless subjected to post-magmatic alteration (Page et al., 2007; Peck et al., 2001), although a variety of geological processes can alter δ^{18}O. Zircon that crystallizes from mantle-derived juvenile magmas has remarkably restricted δ^{18}O values of 5.3 ± 0.6 (2σ) (Valley, 2003; Valley et al., 1998). However, mantle-derived rocks also show subtle variations. For instance, oceanic arc basalts are systematically more enriched in δ^{18}O than MORB owing to the input of subducted lithosphere and sediments that have been modified by low-temperature (near-) surface processes (Woodhead et al., 1987). Zircon δ^{18}O values significantly higher

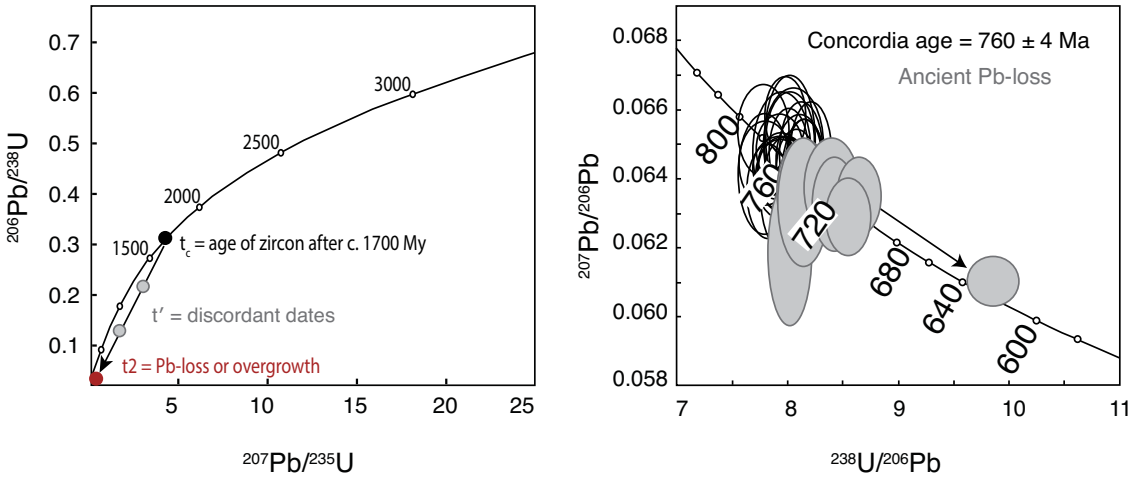

Figure 5. Left: Wetherill concordia diagram showing the history of zircon after ca. 1.7 Gy of radiogenic Pb ingrowth (tc). In this scenario, t2 represents either Pb–loss or new metamorphic overgrowth; t' represents discordant dates subsequent to the tectonomagmatic event at t2. The upper intercept where the discordia line intersects the concordia curve is usually regarded as the age of the sample analyzed, in this case the Pb–Pb dates of the discordia points are identical to the true age of the sample (modified from Schoene, 2014). Right: Tera–Wasserburg inverse concordia diagram depicting ancient Pb–loss and slip along the concordia curve of a sample with a crystallization age of ca. 760 Ma. The youngest concordant date at ca. 630 Ma corresponds to the well–known post–tectonic tectonomagmatic period in the ANS. Recent Pb–loss displaces data points horizontally from the concordia curve because the Pb escaping the system has the same 207Pb/206Pb ratio.

than the mantle range signify input of supracrustal material that experienced low temperature processes such as erosion and sedimentary recycling (Peck et al., 2003; Valley et al., 2005). Zircon $\delta^{18}O$ values that are lower than the pristine mantle values reflect assimilation of high-temperature hydrothermally altered rocks (Bacon et al., 1989), or remelting of such source rocks (Grimes et al., 2013). Non-metamict zircons preserve their $\delta^{18}O$. One useful application of zircon oxygen isotopes is in understanding of sedimentary processes throughout Earth's history. This is essential because it allows recognition of the role of sediment recycling in granitic magmatism through time (Payne et al., 2015; Spencer et al., 2014; Valley et al., 2005; Veizer and Mackenzie, 2014).

4.5. The Sm-Nd isotope system

^{147}Sm undergoes α-decay to produce ^{143}Nd, with a half–life of 106 Ga ($\lambda = 6.54 \times 10^{-12} yr^{-1}$; Dickin, 2005) and forms the basis for the utility of this isotope system. The accumulation of the radiogenic ^{143}Nd is very slow and the $^{143}Nd/^{144}Nd$ ratio increased only by 0.00577 during the 4.5 Ga history of the Earth (Jacobsen and Wasserburg, 1984). Because of this, the Sm–Nd system is well-suited to studies of planetary differentiation. From a planetary perspective, the parent–daughter pairs are unlikely to be fractionated by processes such as condensation of solar nebula because of their highly refractive nature (Depaolo, 2012; McSween and Huss, 2010; Grossman and Larimer, 1974). This coupled with their lithophile nature imply that variations in Sm/Nd ratios are due to silicate (crust–mantle), not core-mantle, differentiation (DePaolo, 2012). Variations in $^{143}Nd/^{144}Nd$ are very small and are therefore expressed relative to a uniform reservoir of the chondritic composition (CHUR) using the ε notation. ε_{Nd} is the relative deviation of the $^{143}Nd/^{144}Nd$ ratios of the sample from the chondritic ratios in parts per 10, 000 (DePaolo and Wasserburg, 1976):

$$\varepsilon_{Nd}(t) = \left[\frac{\left(\frac{^{143}Nd}{^{144}Nd}\right)_{Sample}}{\left(\frac{^{143}Nd}{^{144}Nd}\right)_{CHUR}} - 1 \right] \times 10^4 \quad [6]$$

The utility of the Sm-Nd system in crustal evolution studies stems from the difference in compatibilities of the two elements. The initial $^{143}Nd/^{144}Nd$ ratio of the Earth is the same as that of chondrites or the whole solar system material (White, 2013). Nd is more incompatible than Sm and during partial melting of the mantle Nd is preferentially incorporated into the partial melt and ultimately the crust. This melt extraction leaves the depleted mantle with higher Sm/Nd that evolves along a steeper positive slope and generates crust with lower Sm/Nd ratio that evolves along a shallow slope (Fig. 6). Therefore, over geological time, the crust and mantle attain lower and higher $^{143}Nd/^{144}Nd$ ratios, respectively, and diverge from chondrite (Fig. 6). After crust–mantle differentiation, the Sm/Nd ratio is insensitive

to intracrustal processes and crustal rocks have a uniform $^{147}Sm/^{144}Nd$ ratio of ca. 0.13 (White, 2013). However, the Sm/Nd ratio can be altered by mixing of magmas with different Sm/Nd ratios and in such cases co-genetic samples often form a vertical array in $\varepsilon_{Nd}(t)$ vs. age diagrams (Fig. 6). The undisturbed nature of the Sm/Nd after crustal extraction allows determination of the so-called 'model' age or crustal residence age from measured $^{143}Nd/^{144}Nd$ and $^{147}Sm/^{144}Nd$ ratios provided that sufficient fractionation of Sm/Nd occurs during partial melting of the mantle (Depaolo and Wasserburg, 1976).

4.6. Zircon Lu-Hf isotope systematics

The decay of ^{176}Lu, by β emission with $\lambda = 1.86\times10^{-11}y^{-1}$ (Scherer et al., 2001), produces ^{176}Hf. Both Lu and Hf are refractory lithophile elements. Hf resembles Zr in its crystal chemical behavior and is readily incorporated in the zircon crystal lattice. Apart from being an excellent chronometer mineral, zircon preserve the $^{176}Hf/^{177}Hf$ ratios of the magmas from which they crystalize and is also insensitive to post–crystallization Hf isotope homogenization. The Lu–Hf system is analogous to that of the Sm–Nd scheme in such a way that during mantle melting, the daughter isotope (Hf) is less compatible than Lu and is therefore enriched in the continental crust while the parent Lu is preferentially detained in the depleted mantle (Patchett et al., 1981; Patchett and Tatsumoto, 1980; Vervoort and Patchett, 1996). Therefore, the continental crust evolves towards low $^{176}Hf/^{177}Hf$ while the complementary depleted mantle develops radiogenic (high) $^{176}Hf/^{177}Hf$ ratio (Fig. 7). The Lu–Hf isotopic composition of zircons can, therefore, be used to decipher magmatic evolution in the exact same way as whole-rock Sm–Nd isotope systematics. However, unlike the whole-rock Sm–Nd isotope system which represents the resultant whole-rock composition without textural context, Hf isotopes in zircon can be linked to precise zircon U–Pb ages and $\delta^{18}O$ compositions from the same analytical locations (Griffin et al., 2002; Iizuka et al., 2013; Kemp et al., 2006; Lancaster et al., 2011) and allowing characterization of intra-grain magmatic growth zones. Variations in $^{176}Hf/^{177}Hf$ are expressed relative to CHUR using the epsilon notation at the time of zircon crystallization as:

$$\varepsilon_{Hf}(t) = \left[\frac{\left(\frac{^{176}Hf}{^{177}Hf}\right)_{Sample}}{\left(\frac{^{176}Hf}{^{177}Hf}\right)_{CHUR}} - 1\right] \times 10^4 \quad [7]$$

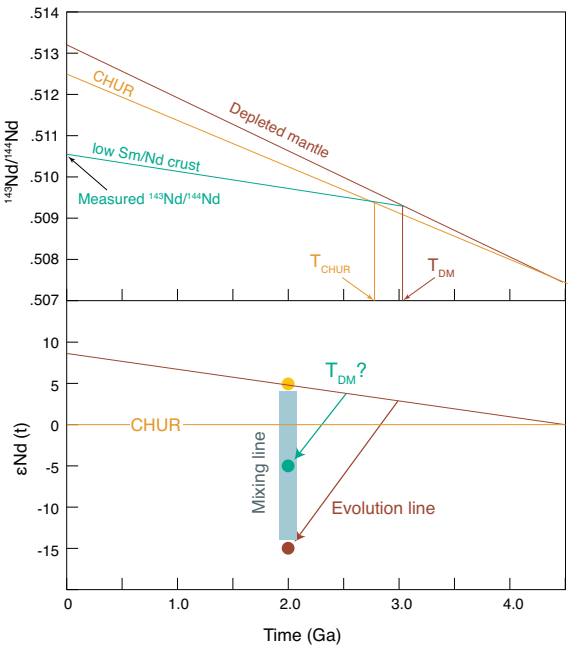

Figure 6. Top: Evolution of Nd isotope ratios in, the chondritic uniform reservoir (CHUR), the perpetually depleted mantle through time and crust. It depicts the model ages obtained by extrapolating the measured $^{143}Nd/^{144}Nd$ back to the assumed model reservoir (DM or CHUR), illustrating the effect of choice of reservoir on model ages (White, 2013). Bottom: The effect of mixing two components (red and yellow points) with different mantle extraction ages on Nd model ages. Any resultant hybrid sample that falls on the mixing line would have a Nd model age that does not correspond to a true geological event and hence called mixed/hybrid model age.

Analogous to the Sm-Nd isotope system, the Lu–Hf system can also be used to estimate crust formation or model ages. A combination of zircon U–Pb ages with Hf model ages from the same analytical location allows evaluation of the relative contributions of juvenile vs reworked crustal additions. If the zircon Hf model age approximates its U–Pb crystallization age (usually within 300 Ma), it is interpreted to represent juvenile magmatic addition. If the Hf model age significantly exceeds the U–Pb age, it is interpreted to represent reworking of ancient crust. Hf model ages are critical in studies of crust-mantle differentiation but the method also has limitations. Hf model ages, like those of Nd model ages, face the problem of mixing two or more sources with different mantle extraction ages and discrepancies arising from the choice of a model reservoir (e.g., depleted mantle vs. island arc; Fig. 7). In the case of mixing, the calculated model ages represent an average crustal residence age which is geologically meaningless as it does not correspond to any particular mantle extraction event (Arndt and Goldstein, 1987). The common approach to circumvent this problem is to filter the Hf isotope data using $\delta^{18}O$ based on the assumption

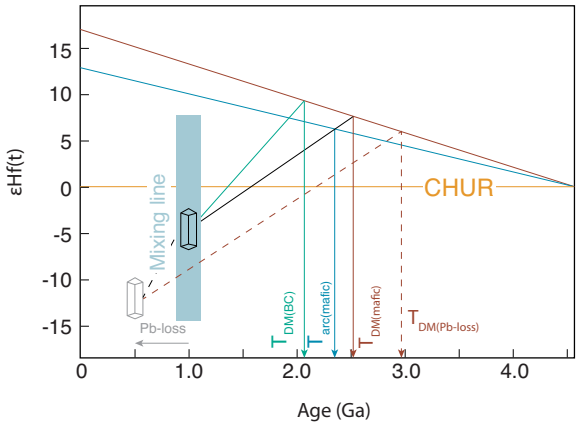

Figure 7. The evolution of Hf isotopes showing the effects of the choice of reservoir, mixing, and Pb-loss on calculated model ages. Modified from Kemp and Hawkesworth (2014).

that zircons with mantle–like $\delta^{18}O$ crystallized from juvenile magmas and therefore calculated Hf model ages are meaningful and zircons with elevated $\delta^{18}O$ crystallized from magmas with crustal input and therefore yield hybrid Hf model ages (Kemp et al., 2006; Lancaster et al., 2011; Pietranik et al., 2008). However, there is an increasing consensus that the reliability of $\delta^{18}O$ in assessing the significance of Hf model ages is hampered by the fact that zircon $\delta^{18}O$ is not sensitive to reworking of ancient crust with mantle-like $\delta^{18}O$ (Kemp and Hawkesworth, 2014; Næraa et al., 2012; Nebel et al., 2011; Payne et al., 2016; Roberts and Spencer, 2014). Another problem with Hf model age calculations is the assignment of reliable crystallization ages that are used in the model age calculations (Whitehouse and Kemp, 2010).

4.7. Secondary ion mass spectrometry (SIMS)

SIMS is a powerful and versatile instrument for *in situ* chemical and isotopic characterization of solid materials. The unique capability of SIMS is its ability to analyze very small portion of the target (5–40 μm in diameter) with a shallow depth of few microns. This high-spatial resolution capability of SIMS allows multiple analyses within single mineral grains and enables isotopic heterogeneities within single grains to be decrypted while preserving petrographic context. The principal components of SIMS are shown in Fig. 8. The most common primary ion source is the duoplasmatron and the primary beam is accelerated through an electrostatic potential. Various lenses and apertures are used to finely focus and/or project the high energy primary ion beam to the sample surface (Ireland, 2014). Ionization yields are highly dependent upon the chemical properties of the primary ion species (Ireland, 2014; Reed, 1989). The most commonly used primary ion species are $^{133}Cs^+$ and $^{16}O^-$ (or $^{16}O_2^-$). To enhance ionization of negative, non-metal secondary ion intensity, strongly electropositive species such as Cs^+ are used as primary ions; for emission of metal secondary ion species such as Pb^+ and UO^+, $^{16}O_n^-$ is used.

The energetic primary ion beam erodes the sample surface and generates a secondary ion spectrum containing both elemental and molecular ions (oxides, multi–oxides and multiply–charged species) which are all transferred to and analyzed in a mass spectrometer (Hinton and Long, 1979). Given such a wide variety of ionized species, an isobaric mass interference, a type of interference that arises whenever another ion with the same nominal mass as the ion of interest is encountered. Such can be resolved with a high mass resolution (Ireland and Williams, 2003b).

Instrumental mass fractionation (IMF), a mass dependent bias that arises during SIMS analyses, undermines the accuracy of SIMS measurements.

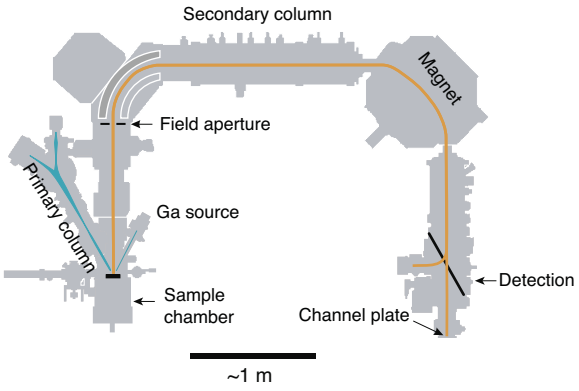

Figure 8. Schematic diagram of CAMECA IMS-1280 secondary ion mass spectrometry (SIMS). Redrawn from Schaltegger et al. (2015).

One utility of chemically and isotopically uniform reference materials is that their measurements can be compared to those of unknown analyses to correct IMF. The reference materials and the unknowns should be matrix–matched, i.e., should have similar compositions as there exists a matrix effect—a compositionally controlled fractionation (Fletcher et al., 2010; Reed, 1989). During the prolonged analytical time (ca. 15 min/spot) in SIMS U-Pb analyses, the combination of unstable primary beam intensity, inter–element fractionations and changing compositions in both the reference zircon and the unknowns are principle limitations on the precision (Ireland and Williams, 2003b; Williams, 1998). In this thesis, SIMS zircon U–Th–Pb analyses for all papers

and O isotope analyses for papers I and IV were performed at the Swedish Museum of Natural History, NordSIMS facility, using a CAMECA IMS–1280.

4.8. Isotope dilution thermal ionization mass spectrometry (ID–TIMS)

The high sensitivity of thermal ionization mass spectrometer (TIMS) makes it a choice of instrument for measurements that require very high precision (Parrish and Noble, 2003). Ionization is achieved by the gradual heating of the filament (usually Re) on which the analyte is placed under vacuum. The main components of TIMS are the ion source, the mass analyzer, ion detectors and ion multipliers. The extracted ions form a beam after passing through successive slits and plates. Since charged particles have different momenta, the focused beam is dispersed into discrete beams having different trajectories according to their charge to mass ratio. Faraday cups collect these beams and convert them to electric current and the ratios of Faraday cups are used to determine isotopic ratios. High–precision isotope measurements by TIMS require effective separation of the analyte elements from the sample matrix. This helps avoid isobaric mass interferences since TIMS are high–sensitivity, low–mass resolution instruments at the expense of textural context. Such chemical separation of the element(s) of interest require longer, days to weeks, times of sample preparation. Compared to other instruments such as SIMS and LA-ICP-MS, the state–of–the–art TIMS instruments have unprecedented sensitivity, precision and sample background for a number of elements of importance in geo/cosmochemistry such as Mg, Cr, Ti, Nd, Os, W and Pb (Ireland, 2014). High levels of precision (<0.005%) on $^{143}Nd/^{144}Nd$ are routinely achievable. The other advantage of TIMS is that cross contamination of samples is minimal; sample contamination, if there is any, often emanates from impurities on the filament and during chemical separation of the elements. There is a strong dependence of the ionization efficiency of TIMS on the ionization potential and the chemical behavior of the element of interest, hindering analyses of some geochemically important elements by TIMS. A good example would be Hf—although the use of Hf isotopes in crust–mantle differentiation studies has long been theoretically established (e.g., Patchett et al., 1981), its application remained limited, as the high ionization potential of Hf made its analysis by TIMS very difficult until the advent of LA–MC–ICP–Ms. All Sm–Nd isotope measurements in this thesis were performed at the Swedish Museum of Natural History using a Thermo Scientific TRITON TIMS instrument.

4.9. LA–MC–ICP–MS

The multicollector inductively coupled plasma mass spectrometer (MC–ICP–MS) was developed to meet the need for more accurate and precise measurements with greater sensitivity required in many areas of research such as geochemistry, cosmochemistry, nuclear, environmental and medical fields (Becker and Dietze, 2000). The strength of the MC–ICP–MS is that its design integrates the superior ionization of the ICP source, even for elements with high (> 95%) first ionization potentials (e.g., Lu, Hf and Fe) that are difficult to analyze using TIMS, with the precise measurements of magnetic sector multicollector mass spectrometer (Walder et al., 1993; Wieser and Schwieters, 2005). Unlike single collector ICP–MS where ions of differing charge to mass ratios (m/z) are sequentially directed to a single detector, MC–ICP–MS instruments enable simultaneous detection of multiple masses using different, up to 12 static and/ movable detectors. Temporal perturbations in the plasma source known as 'flicker noise' during sequential (single–collector) measurements undermine the precision of isotope ratios; whereas the simultaneous collection capability of MC–ICP–MS instruments avoids this transient effect and enables high precision isotope ratio measurements (Jackson et al., 2001; Wieser and Schwieters, 2005). When combined with laser ablation (LA) *in situ* sampling, MC–ICP–MS enables spatially resolvable high precision isotope ratio measurements (Griffin et al., 2000; Kemp et al., 2006). This *in situ* zircon initial Hf isotopic determination using LA–MC–ICP–MS combined with precise U–Pb ages and $\delta^{18}O$ from the same analytical spots/growth zones have provided important insights into crust–mantle differentiation over the past decade. In this thesis (Paper IV), *in situ* zircon Lu–Hf isotope analyses were performed at the National Centre for Isotope Geochemistry, Trinity College Dublin, Ireland using a Thermo–Scientific Neptune MC–ICP–MS coupled to a New Wave 193 nm Excimer LA system.

5. DISCUSSION OF FINDINGS

5.1. The timing and location of a major suture involved in Gondwana assembly

The Precambrian basement rocks of Ethiopia along with the arc–gneiss collage in Yemen are important as they occupy the interface between the low–grade Arabian–Nubian Shield (ANS) to the north and the high–grade, poly-deformed Mozambique Belt (MB) to the south (Fig. 3). Reconnaissance Pb–Pb zircon

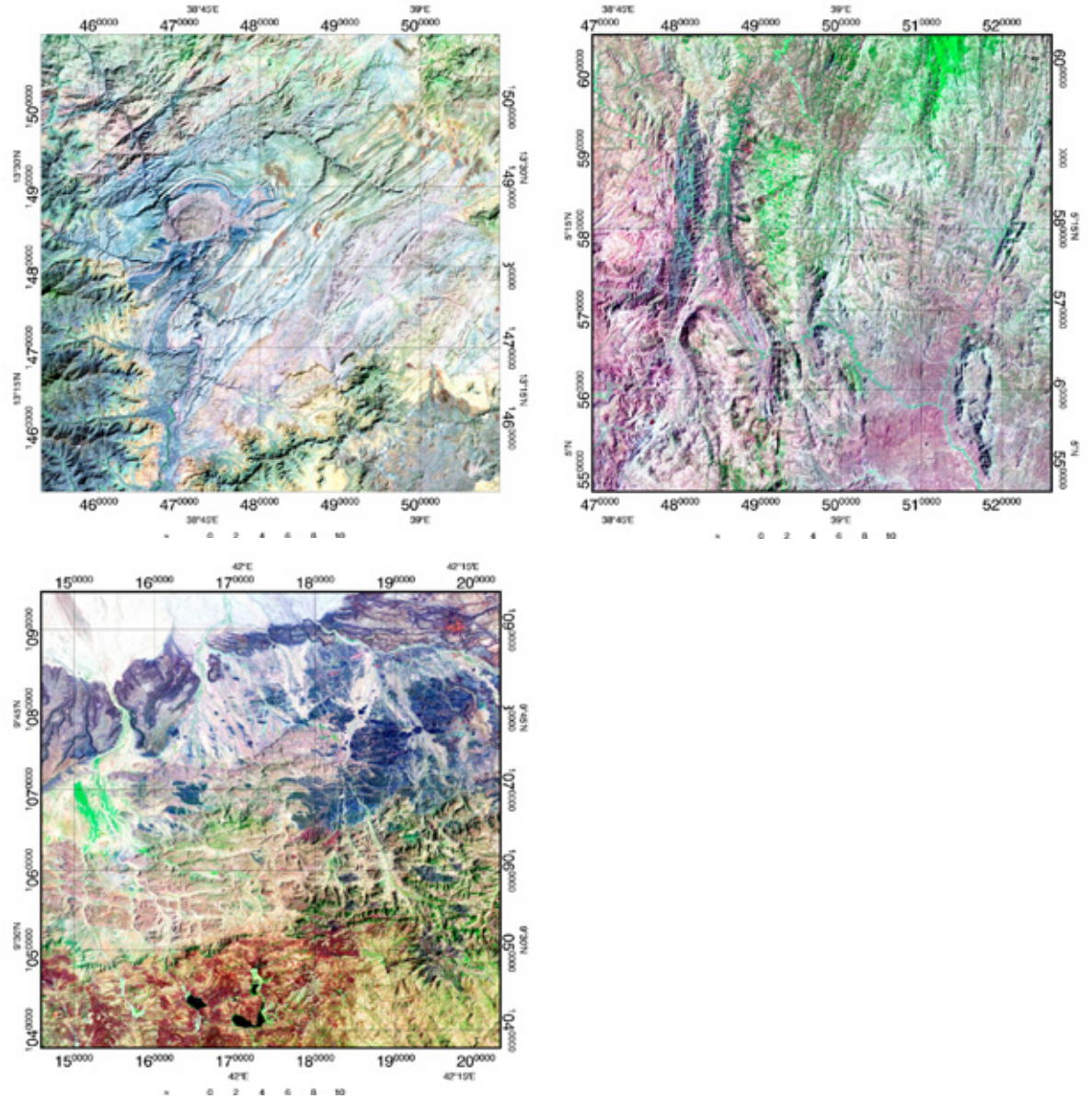

Figure 9. Bands 7–4–2 Landsat Thematic Mapper (TM) imagery showing different structural grains in different parts of Ethiopia. Top left: NNE–trending Precambrian structures in northern Ethiopia. Top right: N–tending structures in southern Ethiopia. Bottom: E–trending structures in the Dire Dawa area (Paper I), eastern Ethiopia.

evaporation analyses of rocks from eastern Ethiopia gave ages as old as ca. 2.8 Ga and their Nd isotope compositions indicate reworking of ancient crust (Teklay et al., 1998). Prior to the opening of the Red Sea and Gulf of Aden ca. 30 Ma ago, the African and Arabian plates were contiguous. It has been suggested that the eastern Ethiopian crystalline basement is part of the Azania micro–continental ribbon that stretches from central Madagascar to Arabia (Collins and Pisarevsky, 2005; Collins and Windley, 2002). Precambrian basement in northern, southern and western Ethiopia have N to NNE trending structures (Fig. 9) and were interpreted to have developed during the assembly of Gondwana. The eastern Ethiopian basement along with the Al–Mahfid terrane of Yemen, however, show an enigmatic E-W structural fabric (Fig. 9). These structural differences, combined with pre–Gulf of Aden reconstructions which put the Dire Dawa basement adjacent to the Archean Al–Mahfid terrane (Silverstein et al., 2012), and the occurrence of late–Archean zircons in both terranes suggest that these two terranes could be correlatives and their east–west structures may have developed prior to the assembly of Gondwana (Silverstein et al., 2012).

In paper I, we conducted a high–spatial resolution SIMS zircon U–Th–Pb, $\delta^{18}O$, and whole–rock Sm–Nd isotope investigation. Despite conscious efforts to characterize any pre–Neoproterozoic zircons, no

Archean or Paleoproterozoic zircons were found. This, coupled with the rounded to sub–rounded morphology of the zircons that yielded pre–Neoproterozoic ages in previous studies (Teklay et al., 1998) and the S–type chemistry of the rocks, suggest that these ancient zircons are likely to be of a sedimentary origin; however, the presence of local Archean to Paleoproterozoic crust cannot be entirely ruled out as sampling in the region is still at a reconnaissance stage. The higher-than-pristine mantle $\delta^{18}O$ values suggest involvement of supracrustal component in the sources of the Dire Dawa granitoids. The exclusively Neoproterozoic crystallization ages contrast with the well–known Archean age of the Al–Mahfid terrane (Whitehouse et al., 1998). These two also have dissimilar Nd model ages: Nd model ages from the Al–Mahfid terrane are late Archean (ca. 3.0–2.7 Ga) and the Dire Dawa crystalline basement yielded model ages in the range 1.7–1.4 Ga. These distinctions suggest that although the two could be structurally correlative, they are isotopically distinct, necessitating a change in age along the length of the Azania microcontinent.

The other major finding of this paper is the identification of two lithospheric blocks in Ethiopia and their timing of amalgamation. It has long been known that pre–existing structures influence the onset and development of ensuing continental rift systems and upper– mantle anisotropy (Corti, 2009; Keranen et al., 2009). Geophysical data point to a change in crustal thickness across the Main Ethiopian Rift (MER), which is interpreted to indicate two distinct lithospheric blocks bounding the MER and these inherited lithospheric structures strongly influenced the onset of rifting in the MER (Keranen and Klemperer, 2008). Nd and Hf isotopic compositions of the Western Ethiopian Shield (WES) indicate that it is juvenile crust (Blades et al., 2015; Woldemichael et al., 2010), in contrast to the Dire Dawa basement which has highly evolved $\varepsilon_{Nd}(t)$ values and ancient model ages. These isotopic differences support the existence of two contrasting lithospheric blocks in Ethiopia, as inferred from geophysical data. Two metamorphic episodes are documented in the WES: one at ca. 635 Ma and a second one at ca. 550 Ma (Ayalew et al., 1990). Zircon metamorphic rim ages from the Dire Dawa samples are ca. 545 Ma, synchronous with the younger metamorphic event in the WES. The absence of the older metamorphic episode in the Dire Dawa basement indicates that by ca. 630 Ma these two lithospheric blocks acted as independent entities. This metamorphic age pattern replicates the one found across a major ca. 580–550 Ma suture extending from Kenya through Madagascar to Antarctica (Boger et al., 2015; Hauzenberger et al., 2007). This ca. 580–550 Ma suture is interpreted as one of the fundamental sutures along which Gondwana assembled (Boger et al., 2015). We interpret the suture between the Dire Dawa basement and WES to be correlative with the one identified further south in Africa and is a major suture formed during the assembly of Gondwana. Importantly, this major suture could have controlled the inception and evolution of the MER.

5.2. Neoproterozoic crust reworking in the Arabian Peninsula and NE Africa

The eastern Ethiopian and Yemen Precambrian rocks represent some of the easternmost exposures in NE Africa and Arabian Peninsula. As such they provide, along with the more distant exposures in Oman (Mercolli et al., 2006; Rantakokko et al., 2014), the only window into the crustal evolution of the region east of the Arabian Shield. In paper II samples collected from traverses across the Abas and Al–Bayda terranes of Yemen and from the Dire Dawa Precambrian basement, eastern Ethiopia, yielded crystallization ages of ca. 790–590 Ma and 790–560 Ma, respectively. Post–tectonic magmatism commenced at ca. 625 Ma, whereas orogenesis continued in the Dire Dawa region until ca. 545 Ma. In post–tectonic settings, magma chemistry commonly evolves from calc–alkaline to alkaline compositions indicating the cessation of orogenesis (Liégeois et al., 1998). In the Abas gneiss and Al-Bayda island arc terranes, calc-alkaline and alkaline magmatism are synchronous at ca. 605 Ma, mark the onset of alkaline magmatism, and indicate that the transition from calc-alkaline to alkaline composition is gradual. Such contemporaneous associations are also observed in post–tectonic plutons of the northernmost ANS (Be'eri-Shlevin et al., 2009).

Post–tectonic plutons elsewhere in the Arabian Shield, however, are remarkably juvenile (Be'eri-Shlevin et al., 2009; Eyal et al., 2010). Compared to the older tectonomagmatic group (ca. 790–730 Ma), the post–tectonic samples have a more radiogenic Nd isotopic composition. This secular variation in $\varepsilon_{Nd}(t)$ points to a diminishing role of pre–Neoproterozoic crustal material and increasing juvenile input, perhaps associated with basaltic underplating in the aftermath of lithospheric root delamination (Avigad and Gvirtzman, 2009). Plutonic rocks from northeast Africa also show highly evolved $\varepsilon_{Nd}(t)$ values (Teklay et al., 1998; Yeshanew et al., 2017), confirming previous observations that this part of the ANS is dominated by reworking of pre-Neoproterozoic crust (Stern, 2002).

The paucity of inherited zircons from the Abas terrane is intriguing given their evolved $\varepsilon_{Nd}(t)$ compositions. The survival of inherited zircons critically depends upon magma temperature and chemistry (Watson and Harrison, 1983). The zircon saturation temperature calculated for the undersaturated samples probably represents a minimum estimate and we interpret the samples to have acquired their evolved $\varepsilon_{Nd}(t)$ composition via deep crustal magma mixing or assimilation.

5.3. Subduction zone or plume–related enrichment?

In paper III, new SIMS U–Pb ages and whole–rock Nd and geochemical data from the southernmost Arabian Shield are used to address this question. In the Arabian Shield, the magmatic axis migrated towards the east or northeast and the oldest arc assemblages are found in southwestern Saudi Arabia. Although it is widely accepted that the shield formed through juvenile magmatic additions through arc accretion in an oceanic realm, some authors (Stein, 2003; Stein and Goldstein, 1996; Teklay et al., 2002) contend that plume material play an important role via accretion of oceanic plateau. About a quarter of the Arabian Shield arc rocks have adakitic affinity (Harris et al., 1993) This implies that the slightly less radiogenic isotopic compositions and trace elements patterns put forward in support of the plume hypothesis could indeed be due to the input of continental material via subduction. Classical adakite rocks were linked to the melting of young and hot slabs (Defant and Drummond, 1990). Since the earliest island arc rocks occur in the southwestern Arabian Shield, the Asir terrane in this part of the shield provides an opportunity to evaluate whether enrichment happened prior to subduction (i.e., plume material) or after subduction (slab component).

The zircon U–Pb data indicate tectonomagmatic events spanning the period ca. 810–610 Ma. The oldest trondhjemite sample (ca. 810 Ma) documents diorite–trondhjemite magmatism prior to 100 Ma in the southernmost Arabian Shield. A granitic gneiss dome emplaced at ca. 770 Ma indicates a change in magma chemistry around that time. Younger diorite–trondhjemite plutonism dated here to ca. 685–665 Ma indicates either such plutons were emplaced over an extended period ca. 810–665 Ma and are contemporaneous with granitic magmatism, or that diorite–trondhjemite magmatism was episodic. The age of the conglomerate clast at 685 ± 3 Ma indicate that locally the plutonic complexes were uplifted and an unconformity developed after ca. 685 Ma. An age of ca. 648 Ma for the oldest post–tectonic sample indicate that post–tectonic magmatism in the southwestern Arabian Shield started slightly earlier compared to the northernmost ANS where post–tectonic calc–alkaline magmatism commenced at ca. 630 Ma (Be'eri-Shlevin et al., 2009).

All samples yield radiogenic $\varepsilon_{Nd}(t)$ compositions, but post–tectonic samples become less radiogenic and have Nd–T_{DM} comparable to the older samples. This suggests a minor involvement of older crustal component in the genesis of the post–tectonic samples. The typical adakitic signatures of the older arc-related samples suggest a possible slab melt as there is no geodynamic evidence for crustal thickening during the arc formation stage in the ANS (Harris et al., 1993). Trace element ratios such as high Ba/La, Ba/Nb and Pb/Ce indicate a sub-arc mantle source metasomatized by slab-derived fluids. The scatter in Ta/Nb ratios of the arc–related samples beyond mantle–derived rocks coupled with their adakite–like chemistry point to an enrichment associated with subduction rather than mantle plume involvement.

5.4. Provenance of the Lower Paleozoic sandstones of the Arabian Shield

Detrital zircon U-Pb, O-, and Hf-isotopic compositions of the Lower Paleozoic sandstones of Saudi Arabia and Jordan indicate continental–scale sediment mixing and dispersal across the northern margin of Gondwana (Paper IV). Subsequent to shield–wide emplacement of post–tectonic granitoids, the ANS experienced erosion and peneplanation, and the underlying crystalline basement became strikingly flat (Garfunkel, 2002; Powers et al., 1966). This continental–scale peneplanation affected the entire Middle East and North Africa and became the platform for the deposition of the vast Cambrian–Ordovician sediments, which are perhaps the largest clastic sedimentary reservoir on Earth (Burke et al., 2003).

This paper is the first study to present a combined detrital zircon *in situ* U–Pb–O–Hf isotopic data on the Cambrian–Ordovician sequences of the ANS. Sample locations from the Saq and Wajid units in Saudi Arabia and Jordan are shown in (Fig. 4b). The age spectra are dominated by ca. 0.9–0.5 Ga and 1.1–0.9 Ga peaks (Fig. 10), with 72.5% and 16.9% respectively. Minor peaks at ca. 3.0 Ga, 2.7–2.5 Ga and 2.2–1.7 Ga are also present (Fig. 10). Zircons older than 2.5 Ga have relatively restricted $\delta^{18}O$ values of 4.0–8.0‰ and younger zircons show wide variations in $\delta^{18}O$ with extreme excursions at ca. 1.0 Ga and 0.7–0.5 Ga. These secular trends in $\delta^{18}O$ in the dataset closely mirror global zircon $\delta^{18}O$ compilations (Spencer et al.,

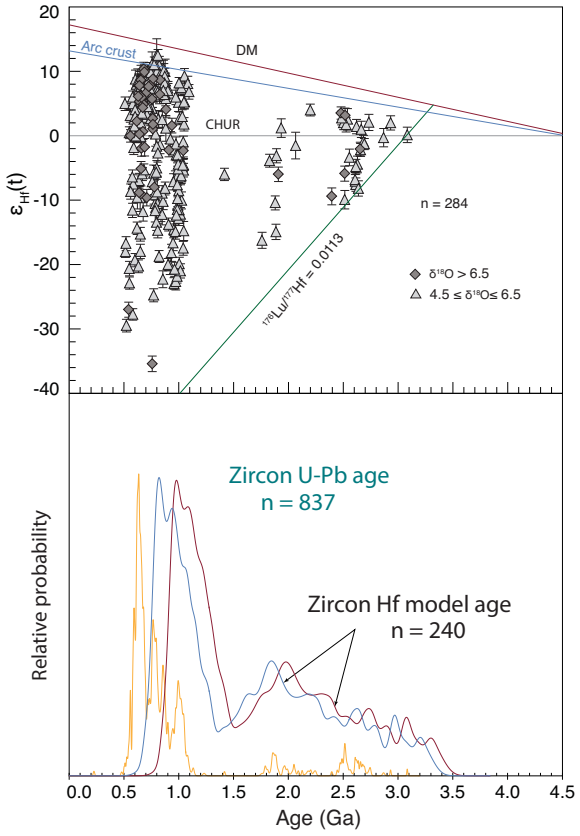

Figure 10. Top: Detrital zircon U–Pb age vs. $\varepsilon_{Hf}(t)$. The green line represents the isotope trajectory of the average continental crust ($^{176}Lu/^{177}Hf = 0.013$, value from Rudnick and Gao, (2013). Bottom: Relative probability distributions of zircon U–Pb and Hf model ages for zircons that are ≥ 90% concordant. Zircon Hf model ages, using the depleted mantle reservoir (red curve) and 'arc crust' (blue curve), were filtered for oxygen isotopic compositions and only those with $4.5<\delta^{18}O<6.5$ are included. Taken from Paper IV.

2014; Valley et al., 2005). Zircons with mantle–like $\delta^{18}O$ values (4.5–6.5‰) show the largest excursions in $\varepsilon_{Hf}(t)$ for the ca. 1.0 Ga and 0.7–0.5 Ga populations, and zircons with non-mantle-like $\delta^{18}O$ values (>6.5‰) have mostly juvenile $\varepsilon_{Hf}(t)$ compositions (Fig. 10). Hf model ages of zircons with mantle-like $\delta^{18}O$ values define two broad peaks at 1.9 Ga and 0.8 Ga (Fig. 10).

About half (47%) of the Neoproterozoic zircons from this study have a juvenile $\varepsilon_{Hf}(t)$ >5 and are interpreted to be sourced from the adjacent juvenile ANS terranes. For the remaining Neoproterozoic zircons with non–juvenile $\varepsilon_{Hf}(t)$ signatures, source regions certainly lie outside of the juvenile ANS terranes. Possible provenance for these are pre–Neoproterozoic terranes reworked during the Neoproterozoic include the arc–gneiss collage of the Precambrian basement of Yemen (Whitehouse et al., 2001, 1998; Windley et al., 1996; Yeshanew et al., 2015), the eastern Ethiopia–northwestern Somalia block (Kröner and Sassi, 1996; Teklay et al., 1998; Yeshanew et al., 2017) and the Mozambique Belt (Kröner and Stern, 2004; Stern, 2002). This is consistent with paleocurrent data which indicates sediment transport from the south (Dabbagh and Rogers, 1983). The second most abundant population at ca. 1.1–0.9 Ga is puzzling since it cannot be attributed to any source terrane known in the region (apart from the ca. 1.1–0.9 Ga zircons of the spatially very restricted Sa'al metamorphic complex in Sinai (Be'eri-Shlevin et al., 2012; Be'eri-Shlevin et al., 2009). Such 1.1–0.9 detrital zircons are generally abundant in the Paleozoic sandstones of North Africa and northern Gondwana (Meinhold et al., 2011; Myrow et al., 2010). Interestingly, these two dominant peaks at ca. 0.7–0.5 Ga and ca. 1.1–0.9 Ga are also present in modern sediments from major African rivers that drain areas where crust with such ages are unknown (Iizuka et al., 2013). These two observations suggest continental–scale mixing and recycling of sediments derived from the EAO mountains and the Kibaran Belt of Central Africa, and dispersal to the periphery of Gondwana. The zircon $\delta^{18}O$ secular variation is consistent with increased incorporation of sediment in the post–Archean magmas and is particularly enhanced by continental collision and crustal thickening (Payne et al., 2015; Valley et al., 2005). The prominent Hf model age peaks at 2.1 Ga and 1.1 Ga are distinct from those found in sediments of East Gondwana at ca. 3.3 Ga and 1.9 Ga (Kemp et al., 2006), indicating that different parts of Gondwana record different growth episodes.

6. CONCLUSIONS

This thesis presents zircon U–Pb geochronological, O and whole–rock Nd isotope data from different parts of the ANS and a combined zircon U–Pb–O–Hf data of the Cambrian–Ordovician sandstone sequences of the ANS. This provides increased understanding of the magmatic evolution and the timing of different tectonomagmatic events in each region and their association with the assembly of Gondwana to be constrained. The principal conclusions are summarized below.

Age and isotopic data from the Dire Dawa Precambrian basement suggest that orogenesis continued in the region until early Cambrian, whereas data from the southernmost Arabian Shield and the Abas terrane in Yemen indicate the culmination of orogenesis by ca. 630 Ma. Reworking of ancient supracrustal material during the Neoproterozoic dominates the evolution of the eastern Ethiopian

basement. It is evident that two contrasting lithospheric blocks exist in Ethiopia—the juvenile Western Ethiopian Shield and the largely reworked pre–Neoproterozoic eastern Ethiopian basement. Metamorphic age distributions in these two domains suggest that the suture between these two lithospheric blocks could represent the northern continuation of a major suture identified further south in Africa associated with the amalgamation of Gondwana and may have controlled the onset and development of the Main Ethiopian Rift. Although the Al–Mahfid terrane of Yemen and the Dire Dawa basement show similar structural grains and plate reconstructions suggest that they are correlative, the data presented here highlights age and isotopic dissimilarities between the two.

The Abas terrane of Yemen represents reworking of pre–Neoproterozoic crust. The paucity of inherited zircons from this pre–Neoproterozoic crustal material could be due to higher zircon saturation temperatures at deeper levels. The Abas has been correlated with the Afif terrane of Saudi Arabia (Collins and Pisarevsky, 2005), but the data presented here again highlights age and isotopic differences, notably the lack of the ca. 1.7 Afif event in the Abas terrane.

The Asir terrane in the southernmost Arabian Shield attests to juvenile magmatic addition. Conservative trace element ratios from the Asir terrane indicate enrichment associated with subduction and lack any plume signature.

The age spectra of the Cambrian–Ordovician sandstones of the ANS are dominated (72.5%) by Neoproterozoic zircons. Slightly more than half of these zircons possess radiogenic Hf isotopic compositions, suggesting the juvenile ANS as a possible source region for these zircons. The remaining unradiogenic population could have been derived from the southern EAO (MB), a region dominated by Neoproterozoic reworking of ancient crust. The large numbers of 1.1–0.9 Ga zircons (17%), combined with the lack of crust of this age being absent from the ANS, suggest derivation from the Grenville-age orogenic zones in Central Africa (Kibaran Belt). This is consistent with paleocurrent indicators which suggest sediment transport from the hinterland of Gondwana. This ubiquity of the 1.1–0.9 Ga age peak across northern Gondwana, and in river sediments in Africa where basements of such age are unknown, suggests that continental–scale sediment mixing/recycling and dispersal was regulated by supercontinent formation. Hf model ages reveal major crust generation episodes at 0.8 Ga and 1.9 Ga. The major growth pulse at 3.3 Ga from eastern Gondwana (Kemp et al., 2006) is lacking from northern Gondwana and suggest that different parts of the supercontinent register different growth episodes.

ACKNOWLEDGEMENTS

First and foremost, I thank Almighty God for keeping me well and for His blessings and favor. I'm most grateful to my supervisors Victoria Pease and Martin Whitehouse for introducing me to the world of isotope geochemistry, for your guidance throughout my project and your intellect. Your insightful comments and feedback on my work are greatly appreciated. I thank my co-authors for their input to the manuscripts, particularly Mohamed Abdelsalam for giving me the chance to work on the eastern Ethiopian samples. I thank Lev Ilyinsky, Kerstin Lindén, Per-Olof Persson, Karin Wallner and Hans Schöberg at NRM for their assistance during my analytical work. Per Andersson is thanked for creating a nice working environment and Kjell Billström for his advice and for helping me settle in Stockholm. I thank everyone I have interacted with at the Department of Geosciences at NRM. At SU, I would like to thank Alasdair Skelton for his suggestions on my thesis; Eve Arnold, Margita Jensen for their handling of administrative issues. Arne Lif at SU and Kristian Eklöf Taavo at NRM are thanked for always swiftly resolving my computer–related problems. Dan Zetterberg for his assistance during sample preparation and his efficiency. The Saudi Geological Survey is thanked for logistical support, especially Mobarak Al Nahdi and Khalid Kadi are thanked for their hospitality and assistance during my field work in Saudi Arabia.

Special thanks go to my parents for their constant support, encouragement and most of all for instilling the love of education in me. My utmost thanks go to my wife Meron Dejene and our lovely daughter Johanna Girum for your love, unwavering support and for your patience and understanding. I'm grateful to my sister Mahider Girum for her encouragement and immense support. My brother and best friend Getenet Reta deserves special thanks for all the fun and friendship. I would like to thank my friends in Ethiopia, Sweden and elsewhere: Fikre Girma, Getu Sintayehu, Fitsum Tadesse, Romuald Rwamamara and his family, Desta H. Hagos, Eyasu Shiferaw, Dagmawit Erike, Samuel Sima, Kidest Mengistu, Jonas Lasskogen, Ditte Kilsgaard Møller and David Whitehead. Last but not least, I would like to express my gratitude to brethren and sisters at our church for the fellowships we had and for their prayers, especially Abrahan Chebude and Bemnet Sintayehu.

REFERENCES

Agar, R.A., 1987. The Najd fault system revisited; a two-way strike-slip orogen in the Saudi Arabian Shield. J. Struct. Geol. 9, 41–48.

Agar, R.A., Stacey, J.S., Whitehouse, M.J., 1992. Evolution of the southern Afif terrane - A geochronologic study. Saudi Arabian Directorate General of Mineral Resources. Open File Report DGMR-OF-10-15, Jiddah, Saudi Arabia.

Ahrens, L.H., 1955. Implications of the Rhodesia age pattern. Geochim. Cosmochim. Acta 8, 1–15.

Albarède, F., 1998. The growth of continental crust. Tectonophysics 296, 1–14.

Ali, B.H., Wilde, S. a., Gabr, M.M. a, 2009. Granitoid evolution in Sinai, Egypt, based on precise SHRIMP U-Pb zircon geochronology. Gondwana Res. 15, 38–48.

Armstrong, R.L., 1981. Radiogenic Isotopes: The Case for Crustal Recycling on a near-steady-state no-continental-growth Earth [and Discussion]. Philos. Trans. R. Soc. A Math. Phys. Eng. Sci. 301, 443–472.

Arndt, N.T., 2013. The Formation and Evolution of the Continental Crust. Geochemical Perspect. 2, 405.

Arndt, N.T., Goldstein, S.L., 1987. Use and abuse of crust-formation ages. Geology 15, 893–895.

Avigad, D., Gvirtzman, Z., 2009. Late Neoproterozoic rise and fall of the northern Arabian-Nubian shield: The role of lithospheric mantle delamination and subsequent thermal subsidence. Tectonophysics 477, 217–228.

Ayalew, T., Bell, K., Moore, J.M., Parrish, R.R., 1990. U-Pb and Rb-Sr geochronology of the Western Ethiopian Shield. Geol. Soc. Am. Bull. 102, 1309–1316.

Bacon, C.R., Adami, L.H., Lanphere, M.A., 1989. Direct evidence for the origin of low-18O silicic magmas: quenched samples of a magma chamber's partially-fused granitoid walls, Crater Lake, Oregon. Earth Planet. Sci. Lett. 96, 199–208.

Be'eri-Shlevin, Y., Eyal, M., Eyal, Y., Whitehouse, M.J., Litvinovsky, B., 2012. The Sa'al volcano-sedimentary complex (Sinai, Egypt): A latest Mesoproterozoic volcanic arc in the northern Arabian Nubian Shield. Geology 40, 403–406.

Be'eri-Shlevin, Y., Katzir, Y., Blichert-Toft, J., Kleinhanns, I.C., Whitehouse, M.J., 2010.

Nd-Sr-Hf-O isotope provinciality in the northernmost Arabian-Nubian Shield: Implications for crustal evolution. Contrib. to Mineral. Petrol. 160, 181–201.

Be'eri-Shlevin, Y., Katzir, Y., Whitehouse, M., 2009. Post-collisional tectonomagmatic evolution in the northern Arabian-Nubian Shield: time constraints from ion-probe U-Pb dating of zircon. J. Geol. Soc. London. 166, 71–85.

Be'eri-Shlevin, Y., Katzir, Y., Whitehouse, M.J., Kleinhanns, I.C., 2009. Contribution of pre-Pan-African crust to formation of the Arabian Nubian shield: New secondary ionization mass spectrometry U-Pb and O studies of zircon. Geology 37, 899–902.

Becker, J.S., Dietze, H.J., 2000. Precise and accurate isotope ratio measurements by ICP-MS. Fresenius. J. Anal. Chem. 368, 23–30.

Belousova, E.A., Kostitsyn, Y.A., Griffin, W.L., Begg, G.C., O'Reilly, S.Y., Pearson, N.J., 2010. The growth of the continental crust: Constraints from zircon Hf-isotope data. Lithos 119, 457–466.

Bentor, Y.K., 1985. The custal evolution of the Arabo-Nubian massif with special reference to the Sinai Peninsula. Precambrian Res. 28, 1–74.

Berhe, S.M., 1990. Ophiolites in Northeast and East Africa: implications for Proterozoic crustal growth. J. Geol. Soc. London. 147, 41–57.

Blades, M.L., Collins, A.S., Foden, J., Payne, J.L., Xu, X., Alemu, T., Woldetinsae, G., Clark, C., Taylor, R.J.M., 2015. Age and hafnium isotopic evolution of the Didesa and Kemashi Domains, western Ethiopia. Precambrian Res. 270, 267–284.

Boger, S.D., Hirdes, W., Ferreira, C.A.M., Jenett, T., Dallwig, R., Fanning, C.M., 2015. The 580–520Ma Gondwana suture of Madagascar and its continuation into Antarctica and Africa. Gondwana Res. 28, 1048–1060

Bowring, S.A., Williams, I.S., 1999. Priscoan (4.00-4.03 Ga) orthogneisses from northwestern Canada. Contrib. to Mineral. Petrol. 134, 3–16.

Bradley, D.C., 2011. Secular trends in the geologic record and the supercontinent cycle. Earth-Science Rev. 108, 16–33

Brown, M., 2007. Metamorphic Conditions in Orogenic Belts: A Record of Secular Change. Int. Geol. Rev. 49, 193–234.

Brown, M., 2006. Duality of thermal regimes is the distinctive characteristic of plate tectonics since the Neoarchean. Geology 34, 961–964.

Burke, K., MacGregor, D.S., Cameron, N.R., 2003. Africa's petroleum systems: four tectonic "Aces" in the past 600 million years, in: Arthur, T.J., MacGregor, D.S., Cameron, N.R. (Eds.), Geological Society, London, Special Publications. pp. 21–60.

Campbell, I.H., Allen, C.M., 2008. Formation of supercontinents linked to increases in atmospheric oxygen. Nat. Geosci. 1, 554–558.

Campbell, I.H., Squire, R.J., 2010. The mountains that triggered the Late Neoproterozoic increase in oxygen: The Second Great Oxidation Event. Geochim. Cosmochim. Acta 74, 4187–4206.

Campbell, I.H., Taylor, S.R., 1983. No water, no granites - no ocean, no continents. Geophys. Res. Lett. 10, 1061–1064.

Canfield, D.E., Poulton, S.W., Narbonne, G.M., 2007. Late-Neoproterozoic Deep-Ocean Oxygenation and the Rise of Animal Life. Science (80-.). 315, 92–95.

Cawood, P.A., Hawkesworth, C.J., Dhuime, B., 2013. The continental record and the generation of continental crust. Bull. Geol. Soc. Am. 125, 14–32.

Cherniak, D.J., Watson, E.B., 2000. Pb diffusion in zircon. Contrib. Miner. Pet. 172, 5–24.

Christensen, N.I., Mooney, W.D., 1995. Seismic velocity structure and composition of the continental crust: A global view. J. Geophys. Res. 100, 9761–9788.

Cogley, J.G., 1984. Continental Margins and the Extent and Number of the Continents. Rev. Geophys. Sp. Phys. 22, 101–122.

Collins, A.S., Pisarevsky, S. a., 2005. Amalgamating eastern Gondwana: The evolution of the Circum-Indian Orogens. Earth-Science Rev. 71, 229–270.

Collins, A.S., Windley, B.F., 2002. The Tectonic Evolution of Central and Northern Madagascar and Its Place in the Final Assembly of Gondwana. J. Geol. 110, 325–339.

Condie, K.C., 2011. Earth as an evolving planetary system. 2nd edition, Elsevier, 559p.

Condie, K.C., 1998. Episodic continental growth and supercontinents: A mantle avalanche connection? Earth Planet. Sci. Lett. 163, 97–108.

Condie, K.C., Aster, R.C., 2010. Episodic zircon age spectra of orogenic granitoids: The supercontinent connection and continental growth. Precambrian Res. 180, 227–236.

Condie, K.C., Belousova, E., Griffin, W.L., Sircombe, K.N., 2009a. Granitoid events in space and time: Constraints from igneous and detrital zircon age spectra. Gondwana Res. 15, 228–242.

Condie, K.C., Bickford, M.E., Aster, R.C., Belousova, E., Scholl, D.W., 2011. Episodic zircon ages, Hf isotopic composition, and the preservation rate of continental crust. Bull. Geol. Soc. Am. 123, 951–957.

Condie, K.C., Kröner, A., Condie, K.C., 2008. When did plate tectonics begin Evidence from the geologic record, in Condie, K. C., and Pease, V., eds., When Did Plate Tectonics Begin on Planet Earth? Geol. Soc. Am. Spec. Pap. 440, 281–294.

Condie, K.C., O'Neill, C., Aster, R.C., 2009b. Evidence and implications for a widespread magmatic shutdown for 250 My on Earth. Earth Planet. Sci. Lett. 282, 294–298.

Condie, K.C., Pease, V., 2008. When Did Plate Tectonics Begin on Planet Earth? Spec. Paper, Geol. Soc. Am. 440, 294p.

Cooper, J.A., Stacey, J.S., Stoeser, D.G., Fleck, R.J., 1979. An Evaluation of the Zircon Method of Isotopic Dating in the Southern Arabian Craton. Contrib. to Mineral. Petrol. 68, 429–439.

Corfu, F., Hanchar, J.M., Hoskin, P.W.O., Kinny, P., 2003. Atlas of zircon textures In: Hanchar, J.M., Hoskin, P.W.O. (Eds.), Zircon. Mineralogical Society of America, in: Hanchar, J.M., Hoskin, P.W.O. (Eds.), Reviews in Mineralogy and Geochemistry. pp. 469–500.

Corti, G., 2009. Continental rift evolution: From rift initiation to incipient break-up in the Main Ethiopian Rift, East Africa. Earth-Science Rev. 96, 1–53.

Dabbagh, M.E., Rogers, J.J.W., 1983. Depositional environments and tectonic significance of the Wajid Sandstone of southern Saudi Arabia. J. African Earth Sci. 1, 47–57.

Defant, M.J., Drummond, M.S., 1990. Derivation of some modern arc magmas by melting of young subducted lithosphere. Nature 374, 662–665.

DePaolo, D.J., 2012. Neodymium isotope geochemistry: An introduction. Springer-Verlag, 187p.

Depaolo, D.J., Wasserburg, G. J., 1976. Nd isotopic variations and petrogenetic models. Geophys. Res. Lett. 3, 249–252.

Dhuime, B., Hawkesworth, C.J., Cawood, P. A., Storey, C.D., 2012. A Change in the Geodynamics of Continental Growth 3 Billion Years Ago. Science. 335, 1334–1336.

Dickin, A.P., 2005. Radiogenic isotope geology. Cambridge University Press, Cambridge, 472p.

Duyverman, H.J., Harris, N.B.W., Hawkesworth, C.J., 1982. Crustal accretion in the Pan African: Nd and Sr isotope evidence from the Arabian Shield. Earth Planet. Sci. Lett. 59, 315–326.

Eyal, M., Litvinovsky, B., Jahn, B.M., Zanvilevich, A., Katzir, Y., 2010. Origin and evolution of post-collisional magmatism: Coeval Neoproterozoic calc-alkaline and alkaline suites of the Sinai Peninsula. Chem. Geol. 269, 153–179.

Faure, G., Mensing, T.M., Faure, G., 2005. Isotopes: Principles and Applications. John Wiley & Sons, 896pp.

Fike, D.A., Grotzinger, J.P., Pratt, L.M., Summons, R.E., 2006. Oxidation of the Ediacaran Ocean. Nature 444, 744–747.

Fleck, R.J., Coleman, R.G., Cornwall, H.R., Greenwood, W.R., Hadley, D.G., Schmidt, D.L., Prinz, W.C., Ratté, J.C., 1976. Geochronology of the Arabian Shield, western Saudi Arabia: K-Ar results. Bull. Geol. Soc. Am. 87, 9–21.

Fleck, R.J., Greenwood, W.R., Hadley, D.G., Anderson, E.R., Schmidt, D.L., 1980. Rubidium-strontium geochronology and plate-tectonic evolution of the southern part of the Arabian Shield. U.S. Geological Survey Professional Paper 1131, 1-36.

Fletcher, I.R., McNaughton, N.J., Davis, W.J., Rasmussen, B., 2010. Matrix effects and calibration limitations in ion probe U-Pb and Th-Pb dating of monazite. Chem. Geol. 270, 31–44.

Flowerdew, M.J., Whitehouse, M.J., Stoeser, D.B., 2013. The Nabitah fault zone, Saudi Arabia: A Pan-African suture separating juvenile oceanic arcs. Precambrian Res. 239, 95–105.

Fyfe, W.S., 1978. The evolution of the Earth's crust: Modern plate tectonics to ancient hot spot tectonics? Chem. Geol. 23, 89–114.

Garfunkel, Z., 2002. Early Paleozoic sediments of NE Africa and Arabia: Products of continental-scale erosion, sediment transport, and deposition. Isr. J. Earth Sci. 51, 135–156.

Goldich, S.S., Fischer, L.B., 1986. Air abrasion experiments in U-Pb dating of zircon. Chem. Geol. Isot. Geosci. Sect. 58, 195–215.

Griffin, W.L., O'Reilly, S.Y., 1987. Is the continental Moho the crust-mantle boundary? Geology 15, 241–244.

Griffin, W.L., Pearson, N.J., Belousova, E., Jackson, S.E., Van Achterbergh, E., O'Reilly, S.Y., Shee, S.R., 2000. The Hf isotope composition of cratonic mantle: LAM-MC-ICPMS analysis of zircon megacrysts in kimberlites. Geochim. Cosmochim. Acta 64, 133–147.

Griffin, W.L., Wang, X., Jackson, S.E., Pearson, N.J., O'Reilly, S.Y., Xu, X., Zhou, X., 2002. Zircon chemistry and magma mixing, SE China: In-situ analysis of Hf isotopes, Tonglu and Pingtan igneous complexes. Lithos 61, 237–269.

Grimes, C.B., Ushikubo, T., Kozdon, R., Valley, J.W., 2013. Perspectives on the origin of plagiogranite in ophiolites from oxygen isotopes in zircon. Lithos 179, 48–66.

Grossman, L., Larimer, J.W., 1974. Early chemical history of the solar system. Rev. Geophys. Sp. Phys. 12, 71–101.

Gurnis, M., Davies, G.F., 1986. Apparent episodic crustal growth arising from a smoothly evolving mantle. Geology 14, 396–399.

Hanchar, J.M., Miller, C.F., 1993. Zircon zonation patterns as revealed by cathodoluminescence and backscattered electron images: Implications for interpretation of complex crustal histories. Chem. Geol. 110, 1–13.

Hargrove, U.S., Stern, R.J., Kimura, J.I., Manton, W.I., Johnson, P.R., 2006. How juvenile is the Arabian-Nubian Shield? Evidence from Nd isotopes and pre-Neoproterozoic inherited zircon in the Bi'r Umq suture zone, Saudi Arabia. Earth Planet. Sci. Lett. 252, 308–326.

Harley, S.L., Kelly, N.M., Möller, A,. 2007. Zircon behaviour and the thermal histories of mountain chains. Elements. 3, 25-30.

Harris, N.B.W., Hawkesworth, C.J., Tindle, A.G., 1993. The growth of continental crust during the Late Proterozoic: geochemical evidence from the Arabian Shield, in: Prichard, H.M., Alabaster, T., Harris, N.B.W., Neary, C.R. (Eds.), pp. 363–371.

Harrison, T.M., Schmitt, A.K., McCulloch, M.T., Lovera, O.M., 2008. Early (≥4.5 Ga) formation of terrestrial crust: Lu-Hf, δ18O, and Ti thermometry results for Hadean zircons. Earth Planet. Sci. Lett. 268, 476–486.

Hauzenberger, C.A., Sommer, H., H., F., Bauernhofer, A., Kröner, A., Hoinkes, G., Wallbrecher, E., Thöni, M., 2007. SHRIMP U – Pb zircon and Sm – Nd garnet ages from the granulite-facies basement of SE Kenya: evidence for Neoproterozoic polycyclic assembly of the. J. Geol. Soc. London. 164, 189–201.

Hawkesworth, C., Cawood, P., Kemp, T., Storey, C., Dhuime, B., 2009. A matter of preservation. Science. 323, 49–50. doi:10.1126/science.1168549

Hawkesworth, C.J., Dhuime, B., Pietranik, A. B., Cawood, P. a., Kemp, a. I.S., Storey, C.D., 2010. The generation and evolution of the continental crust. J. Geol. Soc. London. 167, 229–248.

Hawkesworth, C.J., Kemp, A I.S., 2006. Evolution of the continental crust. Nature 443, 811–817.

Hayward, N.J., Ebinger, C.J., 1996. Variations in the along-axis segmentation of the Afar Rift system. Tectonics 15, 244–257.

Hinthorne, J.R., Andersen, C.A., Conrad, R.L., Lovering, J.F., 1979. Single-grain 207Pb206Pb and U/Pb age determinations with a 10-μm spatial resolution using the ion microprobe mass analyzer (IMMA). Chem. Geol. 25, 271–303.

Hinton, R.W., Long, J.V.P., 1979. High-resolution ion-microprobe measurement of lead isotopes variation within single zircons from Lac Seul, northwestern Ontario. Earth Planet. Sci. Lett. 45, 309–325.

Hoefs, J. Stable Isotope Geochemistry. 7th edition. Springer, 385 p.

Hopkins, M., Harrison, T.M., Manning, C.E., 2008. Low heat flow inferred from 4 Gyr zircons suggests Hadean plate boundary interactions. Nature 456, 493–496.

Hoskin, P.W.O., Schaltegger, U., 2003. The Composition of Zircon and Igneous and Metamorphic Petrogenesis, in: Hanchar, J.M., Hoskin, P.W.O. (Eds.), Zircon. Reviews in Mineralogy and Geochemistry. Mineralogical Society of America, Washing- ton, DC, 27–62. Rev. Mineral. Geochemistry 53, 27–62

Hurley, P.M., 1968. Absolute abundance and distribution of Rb, K and Sr in the earth. Geochim. Cosmochim. Acta 32, 273–283.

Hurley, P.M., Rand, J.R.I., 1969. Science 164, 1229–1242.

Iizuka, T., Campbell, I.H., Allen, C.M., Gill, J.B., Maruyama, S., Makoka, F., 2013. Evolution of the African continental crust as recorded by U-Pb, Lu-Hf and O isotopes in detrital zircons from modern rivers. Geochim. Cosmochim. Acta 107, 96–120.

Ireland, T.R., 2014. Ion Microscopes and Microprobes. In: Analytical Geochemistry/Inorganic INSTR. Analysis. 15, 385-407. Treatise on

Geochemistry: Second Edition. Elsevier Ltd.

Ireland, T.R., Williams, I.S., 2003a. Considerations in Zircon Geochronology by SIMS. Rev. Mineral. Geochemistry 53, 215–241.

Ireland, T.R., Williams, I.S., 2003b. Considerations in Zircon Geochronology by SIMS Zircon. Mineralogical Society of America. Rev. Mineral. Geochemistry 53, 215–241.

Jackson, S.E., Pearson, N.J., Griffin, W.L., 2001. In situ isotoperatio determination using laser ablation (LA)-magnetic sector-ICP-MS, in: P. Sylvester, eds., Laser-Ablation-ICPMS in the Earth Sciences: Principles and Applications, Short Course Series Miner. Assoc. Canada 29, 105–120.

Jacobs, J., Thomas, R.J., 2004. Himalayan-type indenter-escape tectonics model for the southern part of the late Neoproterozoic-early Paleozoic East African-Antarctic orogen. Geology 32, 721–724.

Jacobsen, S.B., Wasserburg, G.J., 1984. Sm - Nd isotopic evolution of chondrites and achondrites, II. Earth Planet. Sci. Lett. 67, 137–150..

Johnson, P.R., Andresen, A., Collins, A. S., Fowler, A. R., Fritz, H., Ghebreab, W., Kusky, T., Stern, R.J., 2011. Late Cryogenian-Ediacaran history of the Arabian-Nubian Shield: A review of depositional, plutonic, structural, and tectonic events in the closing stages of the northern East African Orogen. J. African Earth Sci. 61, 167–232.

Johnson, P.R., Woldehaimanot, B., 2003. Development of the Arabian-Nubian Shield: perspectives on accretion and deformation in the northern East African Orogen and the assembly of Gondwana, in: Yoshida, M., Windley, B.F., Dasgupta, S. (Eds.), Geological Society, London, Special Publications. pp. 289–325.

Kasting, J.F., Catling, D., 2003. Evolution of a habitable planet. Annu. Rev. Astron. Astrophys. 41, 429–463.

Kemp, A.I.S., Hawkesworth, C.J., 2014. Growth and Differentiation of the Continental Crust from Isotope Studies of Accessory Minerals, 2nd ed, Treatise on Geochemistry: Second Edition. Elsevier Ltd.

Kemp, A.I.S., Hawkesworth, C.J., Paterson, B.A., Kinny, P.D., 2006. Episodic growth of the Gondwana supercontinent from hafnium and oxygen isotopes in zircon. Nature 439, 580–583.

Keranen, K., Klemperer, S.L., 2008. Discontinuous and diachronous evolution of the Main Ethiopian Rift: Implications for development of continental rifts. Earth Planet. Sci. Lett. 265, 96–111.

Keranen, K.M., Klemperer, S.L., Julia, J., Lawrence, J.F., Nyblade, A. a., 2009. Low lower crustal velocity across Ethiopia: Is the Main Ethiopian Rift a narrow rift in a hot craton? Geochemistry, Geophys. Geosystems 10.

Kita, N.T., Huberty, J.M., Kozdon, R., Beard, B.L., Valley, J.W., 2011. High-precision SIMS oxygen, sulfur and iron stable isotope analyses of geological materials: Accuracy, surface topography and crystal orientation. Surf. Interface Anal. 43, 427–431.

Kita, N.T., Ushikubo, T., Fu, B., Valley, J.W., 2009. High precision SIMS oxygen isotope analysis and the effect of sample topography. Chem. Geol. 264, 43–57.

Korenaga, J., 2013. Initiation and Evolution of Plate Tectonics on Earth: Theories and Observations. Annu. Rev. Earth Planet. Sci 41, 117–151.

Kranendonk, M.J. Van, Smithies, R.H., Hickman, A.H., Champion, D. C., 2007. Review: secular tectonic evolution of Archean continental crust: interplay between horizontal and vertical processes in the formation of the Pilbara Craton, Australia. Terra Nov. 19, 1–38.

Krogh, T.E., 1982. Improved accuracy of U-Pb zircon dating by selection of more concordant fractions using a high gradient magnetic separation technique. Geochim. Cosmochim. Acta 46, 631–635.

Kröner, A., Stern, R.J., 2004. Pan-African Orogeny. In: Selley, R. C., Cocks, L.R.M., Plimer, I. R. (eds) Encyclopedia of Geology, 1. Elsevier, Amsterdam, 1-12.

Kröner, A., Sassi, F.P., 1996. Evolution of the northern Somali basement: New constraints from zircon ages. J. African Earth Sci. 22, 1–15.

Kusky, T.M., Matsah, M.I., 2003. Neoproterozoic dextral faulting on the Najd Fault System, Saudi Arabia, preceded sinistral faulting and escape tectonics related to closure of the Mozambique Ocean, In Yoshida, M., Windley, B. F., Dasgupta, S., eds., Proterozoic East Gondwana: Supercontin. Geol. Soc. London, Spec. Publ. 206, 327–361.

Lancaster, P.J., Storey, C.D., Hawkesworth, C.J., Dhuime, B., 2011. Understanding the roles of crustal growth and preservation in the detrital zircon record. Earth Planet. Sci. Lett. 305, 405–

412.

Levander, A., Lenardic, A., Karlstrom, K., 2006. Structure of the continental lithosphere. In: Brown, M., Rishmer, T. (Eds.), Evolution and differentiation of the continental crust, Cambridge University Press, cambridge

Li, Z.X., Bogdanova, S. V., Collins, A. S., Davidson, A., De Waele, B., Ernst, R.E., Fitzsimons, I.C.W., Fuck, R. a., Gladkochub, D.P., Jacobs, J., Karlstrom, K.E., Lu, S., Natapov, L.M., Pease, V., Pisarevsky, S. a., Thrane, K., Vernikovsky, V., 2008. Assembly, configuration, and break-up history of Rodinia: A synthesis. Precambrian Res. 160, 179–210.

Liégeois, J.P., Navez, J., Hertogen, J., Black, R., 1998. Contrasting origin of post-collisional high-K calc-alkaline and shoshonitic versus alkaline and peralkaline granitoids. The use of sliding normalization. Lithos 45, 1–28.

Mcguire, A. V, Stern, R.J., 1993. Granulite xenoliths from western Saudi Arabia: the lower crust of the late Precambrian Arabian-Nubian Shield. Contrib. to Mineral. Petrol. 114, 395–408.

McSween, H. Y. Jr., Huss, G. R., 2010. Cosmochemistry. Cambridge University Press, 568p.

Meinhold, G., Morton, A.C., Fanning, C.M., Frei, D., Howard, J.P., Phillips, R.J., Strogen, D., Whitham, A.G., 2011. Evidence from detrital zircons for recycling of Mesoproterozoic and Neoproterozoic crust recorded in Paleozoic and Mesozoic sandstones of southern Libya. Earth Planet. Sci. Lett. 312, 164–175.

Mercolli, I., Briner, A.P., Frei, R., Schönberg, R., Nägler, T.F., Kramers, J., Peters, T., 2006. Lithostratigraphy and geochronology of the Neoproterozoic crystalline basement of Salalah, Dhofar, Sultanate of Oman. Precambrian Res. 145, 182–206.

Meyer, S.E., Passchier, C., Abu-Alam, T., Stüwe, K., 2014. A strike-slip core complex from the Najd fault system, Arabian shield. Terra Nov. 26, 387–394.

Mojzsis, S.J., Harrison, T.M., Pidgeon, R.T., 2001. Oxygen-isotope evidence from ancient zircons for liquid water at the Earth's surface 4,300 Myr ago. Nature 409, 178–181.

Molnar, P., Atwater, T., 1978. Interarc spreading and Cordilleran tectonics as alternates related to the age of subducted oceanic lithosphere. Earth Planet. Sci. Lett. 41, 330–340.

Myrow, P.M., Hughes, N.C., Goodge, J.W., Fanning, C.M., Williams, I.S., Peng, S., Bhargava, O.N., Parcha, S.K., Pogue, K.R., 2010. Extraordinary transport and mixing of sediment across Himalayan central Gondwana during the Cambrian-Ordovician. Bull. Geol. Soc. Am. 122, 1660–1670

Næraa, T., Scherstén, A., Rosing, M.T., Kemp, A. I.S., Hoffmann, J.E., Kokfelt, T.F., Whitehouse, M.J., 2012. Hafnium isotope evidence for a transition in the dynamics of continental growth 3.2 Gyr ago. Nature 485, 627–630.

Nebel, O., Vroon, P.Z., van Westrenen, W., Iizuka, T., Davies, G.R., 2011. The effect of sediment recycling in subduction zones on the Hf isotope character of new arc crust, Banda arc, Indonesia. Earth Planet. Sci. Lett. 303, 240–250.

Nemchin, A. A., Horstwood, M. S. A., Whitehouse, M. J., 2013. High–spatial–resolution geochronology. Elements 9, 31–37.

Page, F.Z., Fu, B., Kita, N.T., Fournelle, J., Spicuzza, M.J., Schulze, D.J., Viljoen, F., Basei, M. a S., Valley, J.W., 2007. Zircons from kimberlite: New insights from oxygen isotopes, trace elements, and Ti in zircon thermometry. Geochim. Cosmochim. Acta 71, 3887–3903.

Pallister, J.S., Stacey, J.S., Fischer, L.B., Premo, W.R., 1987. Arabian Shield ophiolites and Late Proterozoic microplate accretion. Geology 15, 320–323.

Parrish, R.R., Noble, S.R., 2003. 7. Zircon U-Th-Pb geochronology by isotope Dilution — Thermal Ionization Mass Spectrometry (ID-TIMS). Rev. Mineral. Geochemistry 53, 183–213.

Patchett, P.J., Chase, C.G., 2002. Role of transform continental margins in major crustal growth episodes. Geology 30, 39–42.

Patchett, P.J., Tatsumoto, M., 1980. Hafnium isotope variations in oceanic basalts. Geophys. Res. Lett. 7, 1077–1080.

Patchett, P., Kouvo, O., Hedge, C.E., Tatsumoto, M., 1981. Evolution of continental crust and mantle heterogeneity: Evidence from Hf isotopes. Contrib. to Mineral. Petrol. 78, 279–297.

Patriat, P., Achache, J., 1984. India–Eurasia collision chronology has implications for crustal shortening and driving mechanism of plates. Nature 311, 615–621.

Payne, J.L., Hand, M., Pearson, N.J., Barovich, K.M., McInerney, D.J., 2015. Crustal thickening and clay: Controls on O isotope variation in global magmatism and siliclastic sedimentary rocks. Earth Planet. Sci. Lett. 412, 70–76.

Payne, J.L., McInerney, D.J., Barovich, K.M.,

Kirkland, C.L., Pearson, N.J., Hand, M., 2016. Strengths and limitations of zircon Lu-Hf and O isotopes in modelling crustal growth. Lithos 248–251, 175–192.

Pease, V., Johnson, P.R., 2013. Introduction to the JEBEL volume of Precambrian Research. Precambrian Res. 239, 1–5.

Peck, W.H., Valley, J.W., Graham, C.M., 2003. Slow oxygen diffusion rates in igneous zircons from metamorphic rocks. Am. Mineral. 88, 1003–1014.

Peck, W.H., Valley, J.W., Wilde, S. a., Graham, C.M., 2001. Oxygen isotope ratios and rare earth elements in 3.3 to 4.4 Ga zircons: Ion microprobe evidence for high ??18O continental crust and oceans in the early Archean. Geochim. Cosmochim. Acta 65, 4215–4229.

Pietranik, A.B., Hawkesworth, C.J., Storey, C.D., Kemp, A.I.S., Sircombe, K.N., Whitehouse, M.J., Bleeker, W., 2008. Episodic, mafic crust formation from 4.5 to 2.8 Ga: New evidence from detrital zircons, Slave craton, Canada. Geology 36, 875–878.

Powers, R.W., Ramirez, L.F., Redmond, C.D., Elberg, E.L.J., 1966. Geology of the Arabian Peninsula Sedimentary Geology of Saudi Arabia. U.S. Geol. Surv. Prof. Pap. 560–D, 147 p.

Quick, J.E., 1991. Late Proterozoic transpression on the Nabitah fault system—implications for the assembly of the Arabian Shield. Precambrian Res. 53, 119–147.

Ramezani, J., Schmitz, M.D., Davydov, V.I., Bowring, S.A., Snyder, W.S., Northrup, C.J., 2007. High-precision U – Pb zircon age constraints on the Carboniferous – Permian boundary in the southern Urals stratotype. Earth Planet. Sci. Lett. 256, 244–257.

Rantakokko, N.E., Whitehouse, M.J., Pease, V., Windley, B.F., 2014. Neoproterozoic evolution of the eastern Arabian basement based on a refined geochronology of the Marbat region, Sultanate of Oman. Geol. Soc. London, Spec. Publ. 392, 107–127.

Reed, S.J.B., 1989. Ion microprobe analysis a review of geological applications. Mineral. Mag. 53, 3–24.

Reymer, A., Schubert, G., 1986. Rapid growth of some major segments of the continental crust. Geology 14, 299–302.

Reymer, A., Schubert, G., 1984. Phanerozoic addition rates to the continental crust and crustal growth. Tectonics 3, 63–77.

Roberts, N.M.W., Spencer, C.J., 2014. The zircon archive of continent formation through time, In: Roberts, N. M. W., Van Kranendonk, M., Parman, S., Shirey, S., Clift, P. D., eds. Continent formation through time. Geol. Soc. London, Spec. Publ. 389, 197–225.

Rudnick, R.L., 1995. Making continental crust. Nature 378, 571–578.

Rudnick, R.L., Gao, S., 2003. Composition of the Continental Crust. In: Rudnick, R. L. (Ed), The Crust. Treatise on Geochemistry 3, 1–64. Elsevier-Pergamon.

Schaltegger, U., Schmitt, A.K., Horstwood, M.S.A., 2015. U–Th–Pb zircon geochronology by ID-TIMS, SIMS, and laser ablation ICP-MS: Recipes, interpretations, and opportunities. Chem. Geol. 402, 89–110.

Scherer, E., Münker, C., Mezger, K. 2001. Calibration of the lutetium-hafnium clock. Science. 293, 683-687.

Shirey, S.B., Kamber, B.S., Whitehouse, M.J., Mueller, P. a, Basu, A.R., 2008. A review of the isotopic and trace element evidence for mantle and crustal processes in the Hadean and Archean: Implications for the onset of plate tectonic subduction, in Condie, K. C., Pease, V., eds., When Did Plate Tectonics Begin on Planet Earth? Geol. Soc. Am. Spec. Pap. 440, 1–29.

Silverstein, J., Mengesha, L., Yilmu, G., Abdelsalam, M., 2012.Enigmatic regional structural grain of the Precambrian crystalline rocks of Dire Dawa area, Ethiopia. Geological Society of America, Abstracts with Programs, 44, 378.

Spencer, C.J., Cawood, P.A., Hawkesworth, C.J., Raub, T.D., Prave, A.R., Roberts, N.M.W., 2014. Proterozoic onset of crustal reworking and collisional tectonics: Reappraisal of the zircon oxygen isotope record. Geology 42, 451–454.

Squire, R.J., Campbell, I.H., Allen, C.M., Wilson, C.J.L., 2006. Did the Transgondwanan Supermountain trigger the explosive radiation of animals on Earth? Earth Planet. Sci. Lett. 250, 116–133.

Stacey, J.S., Agar, R. a., 1985. U-Pb Isotopic evidence for the accretion of a continental microplate in the Zalm region of the Saudi Arabian Shield. J. Geol. Soc. London. 142, 1189–1203.

Steiger, R.H., Jäger, E., 1977. Subcommission on geochronology: Convention on the use of decay constants in geo- and cosmochronology. Earth Planet. Sci. Lett. 36, 359–362.

Stein, M., 2003. Tracing the plume material in the Arabian-Nubian Shield. Precambrian Res. 123, 223–234.

Stein, M., Goldstein, S.L., 1996. From plume head to continental lithosphere in the Arabian–Nubian shield. Nature. 382, 773-778.

Stein, M., Hofmann, A.W., 1994. Mantle plumes and episodic crustal growth. Nature.

Stern, R.J., 2010. The anatomy and ontogeny of modern intra-oceanic arc systems, in Kusky, T. M., Zhai, M. -G., Xiao, W., eds., The Evolving Continents: Understanding Processes of Continental Growth. Geol. Soc. London, Spec. Publ. 338, 7–34.

Stern, R.J., 2008a. Modern-style plate tectonics began in Neoproterozoic time: An alternative interpretation of Earth's tectonic history, in Condie, K. C., and Pease, V., eds., When Did Plate Tectonics Begin on Planet Earth? Geol. Soc. Am. Spec. Pap. 440, 265–280.

Stern, R.J., 2008b. Neoproterozoic crustal growth: The solid Earth system during a critical episode of Earth history. Gondwana Res. 14, 33–50.

Stern, R.J., 2005. Evidence from ophiolites, blueschists, and ultrahigh-pressure metamorphic terranes that the modern episode of subduction tectonics began in Neoproterozoic time. Geology 33, 557–560.

Stern, R.J., 2002. Crustal evolution in the East African Orogen: A neodymium isotopic perspective. J. African Earth Sci. 34, 109–117.

Stern, R.J., 1994. Arc assembly and continental collision in the Neoproterozoic East African Orogen: Implications for consolidation of Gondwanaland. Annu. Rev. Earth Planet. Sci. 22, 319–351.

Stern, R.J., 1985. The Najd Fault System, Saudi Arabia and Egypt: A late Precambrian rift-related transform system? Tectonics 4, 497–511.

Stern, R.J., Ali, K.A., Ren, M., Jarrar, G.H., Romer, R.L., Leybourne, M.I., Whitehouse, M.J., Ibrahim, K.M., 2016. Cadomian (~560 Ma) crust buried beneath the northern Arabian Peninsula: Mineral, chemical, geochronological, and isotopic constraints from NE Jordan xenoliths. Earth Planet. Sci. Lett. 436, 31–42.

Stern, R.J., Ali, K. a., Liégeois, J.P., Johnson, P.R., Kozdroj, W., Kattan, F.H., 2010. Distribution and significance of pre-neoproterozoic zircons in juvenile neoproterozoic igneous rocks of the arabian-nubian shield. Am. J. Sci. 310, 791–811.

Stern, R.J., Hedge, C.E., 1985. Geochronologic and isotopic constraints on late Precambrian crustal evolution in the Eastern Desert of Egypt.pdf. Am. J. Sci. 285, 97–127.

Stern, R.J., Johnson, P., 2010. Continental lithosphere of the Arabian Plate: A geologic, petrologic, and geophysical synthesis. Earth-Science Rev. 101, 29–67.

Stern, R.J., Johnson, P.R., Kröner, A., Yibas, B., 2004. Neoproterozoic Ophiolites of the Arabian-Nubian Shield, in Kusky, T. M., eds., Precambrian Ophiolites and Related Rocks. Dev. Precambrian Geol. 13, 95–128.

Stern, R.J., Mukherjee, S.K., Miller, N.R., Ali, K., Johnson, P.R., 2013. ~750Ma banded iron formation from the Arabian-Nubian Shield-Implications for understanding neoproterozoic tectonics, volcanism, and climate change. Precambrian Res. 239, 79–94.

Stoeser, B., Stacey, J.S., Greenwood, W.R., Fisher, L.B., 1985. U / PB zircon geochronology of the southern part of the Nabitah mobile belt and Pan-African Continental collision in the Saudi Arabian Shield. Saudi Arabian Deputy Ministry for Mineral Resources Technical Record USGS-TR-04-05.

Stoeser, D.B., Camp, V.E., 1985. Pan-African microplate accretion of the Arabian Shield. Bull. Geol. Soc. Am. 96, 817–826.

Stoeser, D.B., Frost, C.D., 2006. Nd, Pb, Sr, and O isotopic characterization of Saudi Arabian Shield terranes. Chem. Geol. 226, 163–188.

Tang, M., Chen, K., Rudnick, R.L., 2016. Archean upper crust transition from mafic to felsic marks the onset of plate tectonics. Science. 351, 372–375.

Tatsumoto, M., 1970. Age of the Moon: An isotopic study of U-Th-Pb systematics of Apollo 11 Lunar samples-II, Proc. Lunar sci. conf. Geochim. Cosmochim. Acta Suppl. I 1595–1612.

Taylor, S.R., Mclennan, S.M., 1995. TThe geochemical evolution of the continental crust. Rev. Geophys. 33, 241–265.

Teklay, M., Kröner, A., Mezger, K., 2002. Enrichment from plume interaction in the generation of Neoproterozoic arc rocks in northern Eritrea: Implications for crustal accretion in the southern Arabian-Nubian Shield. Chem. Geol. 184, 167–184.

Teklay, M., Kröner, A., Mezger, K., Oberhänsli, R., 1998. Geochemistry, Pb-Pb single zircon ages

and Nd-Sr isotope composition of Precambrian rocks from southern and eastern Ethiopia: implications for crustal evolution in East Africa. J. African Earth Sci. 26, 207–227.

Tera, F., Wasserburg, G.J., 1972. U-Th-Pb systematics in three Apollo 14 basalts and the problem of initial Pb in lunar rocks. Earth Planet. Sci. Lett. 14, 281–304.

Valley, J.W., 2003. Oxygen Isotopes in Zircon In: Hanchar, J.M., Hoskin, P.W.O. (Eds.), Zircon. Mineralogical Society of America. Rev. Mineral. Geochemistry 53, 343–385.

Valley, J.W., Kinny, P.D., Schulze, D.J., Spicuzza, M.J., 1998. Zircon megacrysts from kimberlite: oxygen isotope variability among mantle melts. Contrib. to Mineral. Petrol. 133, 1–11.

Valley, J.W., Lackey, J.S., Cavosie, a. J., Clechenko, C.C., Spicuzza, M.J., Basei, M. a S., Bindeman, I.N., Ferreira, V.P., Sial, a. N., King, E.M., Peck, W.H., Sinha, a. K., Wei, C.S., 2005. 4.4 billion years of crustal maturation: Oxygen isotope ratios of magmatic zircon. Contrib. to Mineral. Petrol. 150, 561–580.

van Hunen, J., van Keken, P.E., Hynes, A., Davies, G.F., 2008. Tectonics of early Earth : Some geodynamic considerations, in Condie, K. C., and Pease, V., eds., When Did Plate Tectonics Begin on Planet Earth? Geol. Soc. Am. Spec. Pap. 440, 157–171.

Veizer, J., Mackenzie, F.T., 2014. Evolution of Sedimentary Rocks, Treatise on Geochemistry: Second Edition.

Vervoort, J.D., Patchett, P.J., 1996. Behavior of hafnium and neodymium isotopes in the crust: Constraints from Precambrian crustally derived granites. Geochim. Cosmochim. Acta 60, 3717–3733.

Walder, A.J., Abell, I.D., Platzner, I., Freedman, P.A., 1993. Lead isotope ratio measurement of NIST 610 glass by laser ablation inductively coupled plasma mass spectrometry. Spectrochim. Acta Part B At. Spectrosc. 48B, 397–402.

Watson, E.B., Harrison, T.M., 1983. Zircon saturation revisited: temperature and composition effects in a variety of crustal magma types. Earth Planet. Sci. Lett. 64, 295–304.

Wetherill, G.W., 1963. Discordant uranium-lead ages: 2. Discordant ages resulting from diffusion of lead and uranium. J. Geophys. Res. 68, 2257–2965.

Wetherill, G.W., 1956. Discordant uranium-lead ages, I. Trans. Am. Geophys. Union 37, 320–326.

White, W.M., 2013. Geochemistry. John Wiley, 670 p.

Whitehouse, M., Stoeser, D.B., Stacey, J.S., 2001. The Khida Terrane - Geochronological and isotopic evidence for Paleoproterozoic and Archean crust in the Eastern Arabian Shield of Saudi Arabia. Gondwana Res. 4, 200–202.

Whitehouse, M.J., Kamber, B.S., Moorbath, S., 1999. Age significance of U-Th-Pb zircon data from early Archaean rocks of west Greenland - a reassessment based on combined ion-microprobe and imaging studies. Chem. Geol. 160, 201–224.

Whitehouse, M.J., Kemp, A.I.S., 2010. On the difficulty of assigning crustal residence, magmatic protolith and metamorphic ages to Lewisian granulites: constraints from combined in situ U-Pb and Lu-Hf isotopes. In: Law, R. D., Butler, R. W. H., Holdsworth, R. E., Krabendam, M., Strachan, R. A. Geol. Soc. London, Spec. Publ. 335, 81–101.

Whitehouse, M.J., Platt, J.P., 2003. Dating high-grade metamorphism—constraints from rare-earth elements in zircon and garnet. Contrib. to Mineral. Petrol. 145, 61–74.

Whitehouse, M.J., Windley, B.F., Ba-Bttat, M. a. O., Fanning, C.M., Rex, D.C., 1998. Crustal evolution and terrane correlation in the eastern Arabian Shield, Yemen: geochronological constraints. J. Geol. Soc. London. 155, 281–295.

Whitehouse, M.J., Windley, B.F., Stoeser, D.B., Al-Khirbash, S., Ba-Bttat, M. a O., Haider, A., 2001. Precambrian basement character of Yemen and correlations with Saudi Arabia and Somalia. Precambrian Res. 105, 357–369.

Wieser, M.E., Schwieters, J.B., 2005. The development of multiple collector mass spectrometry for isotope ratio measurements. Int. J. Mass Spectrom. 242, 97–115.

Wilde, S.A., Valley, J.W., Peck, W.H., Graham, C.M., 2001. Evidence from detrital zircons for the existence of continental crust and oceans on the Earth 4.4 Gyr ago. Nature 409, 175–178.

Williams, I.S., 1998. U-Th-Pb Geochronology by Ion Microprobe, in McKibben, M. A., Shanks III, W. C., Ridley, W. I., eds., Applications of microanalytical techniques to understanding mineralizing processes. Rev. Econ. Geol. 7, 1–35.

Windley, B.F., Whitehouse, M.J., Ba-Bttat, M.A.O., 1996. Early Precambrian gneiss terranes and Pan-African island arcs in Yemen: Crustal

accretion of the eastern Arabian shield. Geology 24, 131–134.

Woldemichael, B.W., Kimura, J.I., Dunkley, D.J., Tani, K., Ohira, H., 2010. SHRIMP U-Pb zircon geochronology and Sr-Nd isotopic systematic of the Neoproterozoic Ghimbi-Nedjo mafic to intermediate intrusions of Western Ethiopia: A record of passive margin magmatism at 855 Ma? Int. J. Earth Sci. 99, 1773–1790.

Woodhead, J.D., Harmon, R.S., Fraser, D.G., 1987. O, S, Sr, and Pb isotope variations In volcanic-rocks from the Northern Mariana Islands - implications for crustal recycling In intra-oceanic arcs. Earth Planet. Sci. Lett . 83, 39–52.

Yeshanew, F.G., Pease, V., Abdelsalam, M.G., Whitehouse, M.J., 2017. Zircon U–Pb ages, δ18O and whole-rock Nd isotopic compositions of the Dire Dawa Precambrian basement, Eastern Ethiopia: Implications for the assembly of Gondwana. J. Geol. Soc. London. 174, 142–156.

Yeshanew, F.G., Pease, V., Whitehouse, M.J., Al-Khirbash, S., 2015. Zircon U-Pb geochronology and Nd isotope systematics of the Abas terrane, Yemen: Implications for Neoproterozoic crust reworking events. Precambrian Res. 267, 106-120.